Energy Conversion and Management 355 (2026) 121244

Contents lists available at ScienceDirect

Energy Conversion and Management

journal homepage: www.elsevier.com/locate/enconman

Research Paper

Modelling, optimization and control of hydrogen-based power supply system for residential buildings

Matic Rutnik *, Boštjan Pregelj, David Jovan, Gregor Dolanc

Department of Systems and Control, Jožef Stefan Institute, Jamova cesta 39, 1000 Ljubljana, Slovenia

ARTICLE INFO

Keywords:
Hydrogen technologies
Energy storage
Renewable power
Residential building
Optimal sizing
Power management

ABSTRACT

This paper analyses a self-sustained, green electricity supply system for residential buildings based on photovoltaic generation supported by battery and hydrogen energy storage. Photovoltaic power generation depends on season, time of day, and weather, and is inherently out of sync with residential electricity demand. This imbalance can be addressed through short-term storage using batteries and long-term storage using a hydrogen system composed of an electrolyser, hydrogen storage, and a fuel cell. However, the high cost of technological equipment results in high annual costs of electricity and heat supply, making optimal system design and operation essential. To address this challenge, a techno-economic simulation model of the entire system is developed to support optimal component sizing and process control. Compared to related studies, the proposed approach employs simple and transparent techno-economic models, enabling adaptability to specific use cases. A power management algorithm is introduced to prioritise battery-based daily balancing and hydrogen-based seasonal balancing. The simulation study provides full-year energy flow profiles, detailed annual energy balance results, and a breakdown of electricity supply costs. Thermal integration of the fuel cell and heat pump is also considered to improve overall system efficiency. Results indicate that, with appropriate sizing and control, the annual electricity supply cost is approximately 4300 EUR for a state-of-the-art single-family house, which may be competitive in regions with high electricity and transmission costs.

1. Introduction

To protect the environment, reduce greenhouse gas emissions, and decrease dependence on fuel suppliers, the use of fossil fuels must be reduced and replaced by renewable power sources such as photovoltaic, wind, and hydropower. All areas, including industry, mobility, transportation, as well as commercial and residential buildings, are subject to the green transition. One of the greatest challenges of renewable power sources is their dependence on weather. Their power generation varies with the season, time of day, and current weather conditions, which by default does not match the actual power demands of industry, transportation, and buildings. In general, different strategies can be used to address this problem, one of which is energy storage. In this approach, surpluses of renewable energy are stored and later used during periods when there is a shortage of energy, i.e., when energy consumption exceeds generation. Options for storing renewable electric energy are very limited and come with technical and economic challenges. Batteries, for example, can store relatively small amounts of energy over short periods, i.e., several hours or days. For larger amounts and longer periods, hydrogen technologies can be used, but these also face technical issues and high costs [1]. Using hydrogen technologies, surpluses of renewable energy can be converted into hydrogen by water electrolysis. The generated hydrogen can then be stored in various forms (pressurised, liquid, or chemical storage). During periods of electric energy shortage, stored hydrogen can be converted back to electricity and heat by fuel cells. This technology can be used in different areas, in various configurations, and at different scales. This paper focuses on the electric power and heat supply of buildings, typically residential buildings, such as family houses and households [2].

The main motivation for this study stems from several significant changes in building construction legislation and in the accounting of electricity consumption and production, which are expected soon: (1) the obligation to install photovoltaic panels on new and renovated buildings, (2) restrictions on the use of fossil fuels for heating in new buildings [3], (3) a sharp increase in electric energy transmission fees, and (4) changes in net metering for electricity generated by local renewable sources, such as rooftop photovoltaic (PV) panels. These new conditions are expected to significantly increase the demand for at least partial energy self-sufficiency in residential buildings. This requires not

* Corresponding author.
E-mail address: matic.rutnik@ijs.si (M. Rutnik).

https://doi.org/10.1016/j.enconman.2026.121244
Received 28 October 2025; Received in revised form 11 February 2026; Accepted 15 February 2026
Available online 4 March 2026

Nomenclature

Symbol	Description (Unit)
General parameters	
t	Time of year (day of year, time of day) (–)
R	Gas constant (8.314) (J/(mol K))
T	Absolute temperature in the hydrogen tank (K)
Photovoltaic (PV) system	
J_S	Solar radiation at given time of year (W/m^2)
A	Photovoltaic power plant area (m^2)
μ	Photovoltaic power plant efficiency, i.e. ratio between sun radiation (W/m^2) and generated electric power (W/m^2); assumed value is 0.1 (10 %), but it depends on photovoltaic panel type, age, mounting orientation and ambient temperature. (–)
P_{PV}	Photovoltaic power plant, generated electric power (kW)
Consumers and grid	
P_C	Power of electrical consumers (all except the heat pump) (kW)
P_E	The difference between the generated electric power (P_{PV}) and the consumed electric power ($P_C + P_{HP\_E}$) (kW)
P_{G_IN}	Grid input power (kW)
P_{G_OUT}	Grid output power (kW)
Electrolyser (EL)	
P_{EL_IN}	Electrolyser, input power (kW)
P_{EL_E}	Electrolyser, input electric power (kW)
P_{EL_H2}	Electrolyser, output power of the generated hydrogen (kW)
ϕ_{EL_H2}	Electrolyser, mass flow rate of the generated hydrogen (kg/s)
P_{EL_MIN}	Electrolyser minimum threshold operation power (kW)
P_{EL_T}	Electrolyser, thermal power due to losses (kW)
η_{EL}	Electrolyser, energy efficiency (see Fig. 8)
Fuel cell (FC)	
P_{FC_H2}	Fuel cell, input power of consumed hydrogen (kW)
P_{FC_E}	Fuel cell, output electric power (kW)
P_{FC_T}	Fuel cell, thermal power due to losses (kW)
P_{FC_OUT}	Fuel cell output power (kW)
ϕ_{FC_H2}	Fuel cell, mass flow rate of consumed hydrogen (kg/s)
η_{FC}	Fuel cell, energy efficiency (see Fig. 10)
Hydrogen (H2) storage	
m	Mass of the hydrogen in the tank (kg)
M	Molar mass of the hydrogen (2.01568 x 10^{-3}) (kg)
n	Number of moles of hydrogen in the hydrogen tank
E_{H2}	Energy of the hydrogen in the tank (kWh)
E_{H2_MAX}	Maximal energy of the hydrogen in the tank (kWh)
E_{H2_MIN}	Minimal energy of the hydrogen in the tank (kWh)
E_{H2_INIT}	Energy of the hydrogen in the tank, initial value (kWh)
HHV	High heating value of hydrogen (39.39 kWh/kg) (kWh/kg)
p	Pressure in the hydrogen tank (Pa)
p_{max}	Maximal pressure in the hydrogen tank (Pa)
V	Geometric volume (m^3)
V_T	Geometric volume of the hydrogen tank (m^3)
T_F	Tank full
T_E	Tank empty
Battery (B)	
P_{B_IN}	Battery charging power (kW)
P_{B_OUT}	Battery reduced discharging power (kW)
$P_{B\_IN\_MAX}$	Battery maximum charging power (kW)
$P_{B\_OUT\_MAX}$	Battery maximum discharging power (kW)
$P_{B\_IN\_L}$	Battery charging losses power (kW)
$P_{B\_OUT\_L}$	Battery discharging losses power (kW)
$P_{B\_IN\_C}$	Battery reduced charging power (kW)
$P_{B\_OUT\_D}$	Battery discharging power (kW)
E_B	Energy of the battery (kWh)
E_{B_INIT}	Energy of the battery, initial value (kWh)
η_C	Battery charging efficiency (typically 95 %)
η_D	Battery discharging efficiency (typically 95 %)
E_{B_MAX}	Battery capacity (kWh)
E_{B_MIN}	Battery lower defined capacity (kWh)
B_F	Battery full
B_E	Battery empty
Heat pump (HP) and thermal storage	
P_{HP_E}	Heat pump, consumed electric power (kW)
P_{HP_T}	Heat pump, generated thermal power (kW)
$P_{HP\_T\_min}$	Heat pump, minimum generated thermal power (kW)
$P_{HP\_T\_max}$	Heat pump, maximum generated thermal power (kW)
$P_{HP\_T\_DEM}$	Demanded thermal power of the heat pump (kW)
P_T	Total generated thermal power, i.e. heat pump + fuel cell losses (kW)
P_{T_DEM}	Total demanded heating power (kW)
CoP_{HP}	Coefficient of Performance of heat pump (ratio between thermal and electric power), assumed 3.0
CTRL	Heat storage control for heat pump
E_{ST_SET}	Stored heat in thermal storage – setpoint (kWh)
E_{ST_ACT}	Stored heat in thermal storage – actual (kWh)
e	Stored heat – control error (kWh)
e_{min}	Control error min., corresponds to the min. thermal power of the heat pump (kWh)
e_{max}	Control error max., corresponds to the max. thermal power of the heat pump (kWh)
Economic and technical parameters	
EP_{PV}	Price component, PV power plant (EUR)
EP_{BATT}	Price component, battery (EUR)
EP_{EL}	Price component, electrolyser (EUR)
EP_{FC}	Price component, fuel cell (EUR)
EP_{H2_STOR}	Price component, hydrogen storage
t_{L_X}	Expected lifetime of particular element (year)
Abbreviations	
PV	Photovoltaic
BATT	Battery
EL	Electrolyser
FC	Fuel cell
H2_STOR	Hydrogen storage
CONS	Others consumers
HP	Heat pump

only the use of local renewable energy sources but also both short-term and long-term (e.g., seasonal) energy storage. The need for local storage arises from two main factors. First, under the new net metering rules [4], the energy balance will be calculated monthly instead of yearly, meaning surplus energy generated in summer will no longer offset winter deficits. Second, higher transmission fees will impose additional costs on renewable energy owners for daily exchanges with the grid. Both challenges can be addressed by local energy storage, but this involves high costs for technological equipment (batteries and hydrogen technology equipment). The resulting price of local energy supply can be high, making investment in such a system unattractive.

To minimise investment and energy supply costs, the local energy

system must be optimally sized during design and optimally managed and controlled during operation. Avoiding oversizing and selecting the appropriate combination of component sizes are essential for reducing costs. This paper focuses on the techno-economic mathematical modelling and simulation of a local energy supply and storage system based on PV energy, supported by battery and hydrogen-based storage. The ultimate goal is to develop a simulation model of the entire system that can serve as a design and decision support tool to identify the optimal configuration of system parameters for achieving the lowest possible energy supply cost for a given energy generation and consumption profile. Given the nonlinearities and the number of parameters involved, the optimal solution cannot be derived analytically but can be approximated using simulation-based methods.

Due to its importance, this topic has been extensively addressed. The literature provides a general overview, as well as the technical feasibility, opportunities, and challenges of local energy systems based on hydrogen and battery storage.

For example, the fundamental properties of battery-based short-term storage and hydrogen-based long-term storage, including heat utilisation, are detailed in [9], and their application is demonstrated through a hybrid battery–hydrogen system case study in Central Europe. In [5], a system for residential applications based on wind turbines, photovoltaic panels, and hydrogen is presented and analysed using the HOMER tool. Reference [6] examines an off-grid, self-sustained residential house equipped with photovoltaic panels, a battery, an electrolyser, hydrogen storage, and a fuel cell. Study [7] considers a prosumer system, based on photovoltaic panels, a battery, and hydrogen system, which is connected to a local electric vehicle charging station and can also connect to the electric grid to trade electric energy. Another example [8] optimises off-grid hybrid renewable energy systems using ε-constraint and particle swarm optimisation to minimise the levelised cost of energy and CO_2 emissions. The results highlight hydrogen storage as a key enabler of high renewable penetration, reducing the levelised cost of energy (LCOE) by up to 35 % compared to battery-only systems. Reference [10] demonstrates the technical feasibility and economic viability of a fully renewable, multi-sector global energy system, emphasising the role of electrification and hydrogen-based sector coupling in achieving a cost-effective, sustainable, and secure energy supply.

Sizing of local energy systems (optimising sizes and capacities of components) is an area of intense research. The problem is addressed using various techno-economic models that predict system operational and economic performance, as well as a range of optimisation techniques. One early study [11] describes the structure of a typical local energy system (PV power plant, fuel cell, electrolyser, hydrogen storage, and battery) and provides basic principles and guidelines for component sizing. Sizing can be supported computationally using commercial software for modelling and optimisation. In [12], MATLAB Simulink Design Optimization and evolutionary algorithms are used to minimise annual costs while meeting energy needs. In [13], the HOMER software is used for optimal sizing of a photovoltaic plant, fuel cell, electrolyser, hydrogen tank, and battery for a single-family house and a multi-family building, aiming to minimise both electricity and total system cost. Paper [14] presents a model-based exhaustive optimisation method, evaluating all possible combinations of fuel cell and electrolyser sizes. In [15], different evolutionary optimisation algorithms (particle swarm, simulated annealing, tabu search) are used for system sizing and compared. The use of mixed-integer linear programming for local energy system sizing is discussed in [16]. Another case [17] focuses on modelling and sizing the local energy system, with an emphasis on PV modelling. Furthermore, optimisation using simulated annealing is detailed in [18] and fuzzy logic in [19]. In [20], a distributed optimisation algorithm based on the alternating direction method of multipliers (ADMM) is proposed to address the complexity of optimisation when many parameters are subject to optimisation. Optimisation of energy systems for entire energy communities, rather than individual buildings, is addressed in [21] and [22]. A comprehensive overview of recent studies on hybrid energy systems for on-grid and off-grid residential applications is provided in [23].

To optimise system operation, equipment utilisation, and energy supply costs for the user, online control and power management are crucial; therefore, many different approaches are presented in the literature. When only one energy storage device is present in the system, the control algorithm can be very simple (e.g. [24]), as excesses and shortages of local renewable power are compensated by a single energy storage unit. The situation becomes much more complex when there is more than one energy storage device (typically a hydrogen system and batteries) or when there is interaction with the electric grid (on-grid systems). In these cases, different energy management options arise, and various criteria functions must be optimised. Simple control strategies to manage storage in the battery and hydrogen system are presented in [25] and [26]. In [27], an advanced control method is presented that uses model predictive control and mathematical models to optimise energy use under variable electricity pricing improving grid interaction and financial viability. Artificial intelligence methods, such as neural networks and genetic algorithms, have also shown promise for prediction and optimisation in local hydrogen-based systems [28]. In [29], nonlinear optimisation algorithms are used to find the optimal energy plan for a one-day period. In [30], a control system is presented that coordinates the use of local hydrogen-based energy storage and supports the sharing of energy resources between several buildings.

Energy systems based on local PV power and local energy storage can also be developed for multiple residential houses integrated into microgrids [31]. An example of such a centralised energy system is discussed in [32], which uses a reversible solid oxide fuel cell/electrolyser, offering improved energy efficiency and a simplified setup with reduced costs, as the fuel cell and electrolyser are combined into a single reversible device. While serving residential districts and microgrids, hydrogen-based systems can also provide services to the public grid, such as demand response, to further enhance financial viability [33]. Additionally, the integration of electric vehicles, hydrogen, and renewable energy in CHP microgrids has been explored in [34]. Studies [35] and [36] investigate and optimise the combination of fuel cells and Organic Rankine Cycle engines to assess overall system efficiency by utilising fuel cell thermal losses.

Hydrogen storage is a key enabling technology not only for the local energy systems discussed in this paper but also for the broader hydrogen economy. Long-term hydrogen storage presents both technological and economic challenges, which are extensively discussed in [37]. The reviewed literature highlights the complex nature of renewable energy system design and optimisation. It emphasises the importance of technological innovation, policy support, and tailored solutions in addressing the challenges of the energy transition and sustainability.

Many studies in the literature are related to this paper, but detailed analysis reveals considerable differences in underlying system architectures, operation modes, design goals, modelling approaches, control strategies, performance metrics, and representations of results. Therefore, direct comparison of approaches is not straightforward and is sometimes not possible. For example, study [12] assumes a similar system setup (PV, electrolyser, fuel cell, hydrogen storage, battery), similar modelling principles, a simulation duration of one year, and addresses electricity demand but not heat demand or the related thermal integration of the fuel cell and heat pump. In, addition, the daily time profile of the demanded electric power is constant throughout the year, and the differences in daily time profiles of PV-generated energy are modest due to the geographical location of the use case. As a result, seasonal energy storage is not addressed, leading to different control algorithms and different ratios between battery and hydrogen storage capacities compared to this paper. Another similar example is [13], where modelling and optimisation are performed using the HOMER software, which employs built-in models of the components (PV, electrolyser, fuel cell, hydrogen storage, battery, control). The study does

not explain the yearly energy balance in detail, and the data are presented only on a monthly basis. There is also no utilisation of fuel cell thermal losses for heating purposes. Paper [42] addresses the utilisation of fuel cell waste heat to reduce the load on the heat pump, but the overall system architecture differs from that used in this paper, as there is no local PV plant or electrolyser. Study [43] also addresses the utilisation of dissipated heat from the fuel cell, but the heating source is a CHP boiler rather than a heat pump, so the system structure is different. Another recent example is [44], which assumes a similar system setup for residential houses but lacks hydrogen storage and thermal storage. A further recent case [49] proposes and analyses a residential house power system based on a fuel cell that meets electric, heating, and cooling demands, with hydrogen generated off-site and purchased at a competitive price.

The added value of this work is in integrated and systematic analysis of a self-sustained residential energy system. The paper combines transparent techno-economic models of commercially available components with real, high-resolution generation and consumption data, including degradation effects of electrochemical devices, to enable simulation over entire year under realistic operating conditions. An important aspect of the work is an automated control strategy that separates short-term (daily) energy balancing, handled by batteries, from long-term (seasonal) balancing, handled by hydrogen storage. The interaction between the electrical subsystem and thermal subsystem (heat pump) is further examined through the thermal integration of fuel cell waste heat with a heat pump, allowing the impact on electricity consumption and system sizing to be assessed.

Beyond energy performance, the study provides component-level attribution of annual electricity and heat supply costs and evaluates multiple system configurations, revealing that energy supply cost-optimal designs do not necessarily align with those achieving maximum energy efficiency, and identifying hydrogen storage as a dominant cost driver under current assumptions. Together, these elements offer design-oriented insight into the techno-economic trade-offs of residential hybrid battery-hydrogen energy systems, which are not typically addressed jointly in existing literature.

The paper is organised as follows. Section 2 describes the local energy system, and Section 3 develops its model. An important part of the system is the power management algorithm, explained in Section 4. The generated techno-economic model is used for a simulation study, with results and commentary presented in Section 5.

2. System description

The local energy system is shown in Fig. 1.

A photovoltaic (PV) power plant provides green, and carbon-free electric energy for all electrical consumers, including the heat pump. The electrolyser converts temporary surpluses of electric power into hydrogen, with most surpluses occurring during the daytime in summer. The hydrogen storage tank stores the generated hydrogen in pressurised gaseous form. As hydrogen has a very low density (0.09 kg/m^3), it must be pressurised to keep the geometric size of the storage tank acceptable. Typical pressures are 20–100 bar in larger industrial tanks and 300–700 bar in smaller automotive tanks. The electrolyser can generate hydrogen at pressures up to 50 bar. If higher storage pressure is required, a hydrogen compressor must be added to the system. The fuel cell converts the stored hydrogen back into electric energy and heat when the electric energy produced by the PV power plant does not meet the demand, typically during the night and in winter. The energy efficiency of the fuel cell is around 60 %, meaning approximately 40 % of the hydrogen's energy is not converted into electricity, but into heat, which can be used for building and sanitary water heating. The battery is an optional part of the system and can be used for short-term storage of surplus electric energy generated during the day for use at night. Although the battery represents an additional cost, it can reduce overall costs by decreasing the size and cost of the electrolyser and the energy losses associated with converting electric energy into hydrogen and back. **Consumers other** represent all devices and appliances that use electric energy (air conditioning, ventilation, lighting, infotainment and entertainment devices, kitchen appliances, and similar), except the heat pump, which is considered separately. **The heat pump** for building and sanitary water heating is the major electricity consumer. The electricity consumption of the heat pump can be significantly reduced if the waste heat from the fuel cell is used for heating. **Heat storage** acts as a buffer to balance heat generation (by the heat pump and fuel cell losses) and heat demand (building and sanitary water heating). Heat is stored in an ideally insulated liquid (typically water) tank. In the context of self-sufficiency, **the grid** is an auxiliary part of the energy supply system. It absorbs possible surpluses of electric energy that cannot be stored due to battery and hydrogen system limitations (Table 1). Furthermore, the grid supplies electric energy in case of failures in the local energy supply system and in the undesirable case when the energy stored in the battery and hydrogen system is depleted. The design goal is to minimise energy flow to and from the grid.

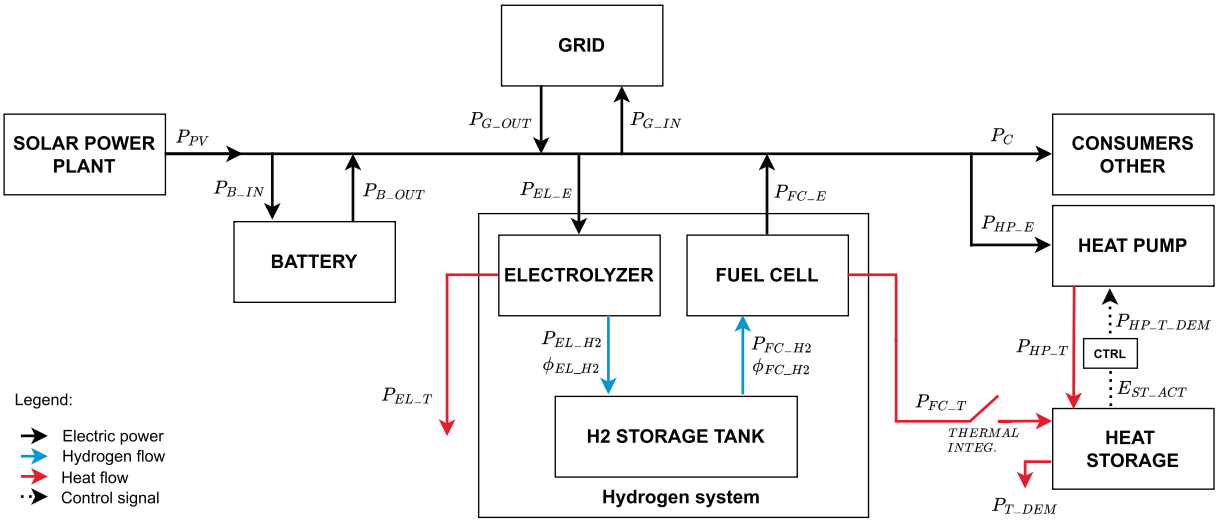

Fig. 1. System configuration.

Table 1
Main parameters of the system.

Parameter	Value
Fuel cell efficiency (η_{FC})	app. 60 %
Electrolyser efficiency (η_{EL})	app. 70 %
Hydrogen storage pressure maximum (p_{max})	50 bar
Battery charging efficiency (η_C)	95 %
Battery discharging efficiency (η_D)	95 %
Heat pump coeff. of performance (CoP_{HP})	3.0

3. System model

For simulation and optimisation purposes, a model of the entire system is developed and implemented as a MATLAB script.

3.1. Photovoltaic power plant model

The model of the PV power plant predicts the generated electric power as a function of time throughout the year. The amount of power generated is proportional to the surface area of the PV plant, its efficiency, and solar radiation power at a given time of year. The solar radiation power received, J_S, is affected by factors such as weather conditions, the micro-location of the power plant, and the time of year (Fig. 2). The model does not account for the effect of temperature on PV efficiency.

In reality, the received solar power strongly depends on the tilt angle and orientation (azimuth) of PV panels. In this study, horizontal mounting (tilt angle 0°) is assumed, for which the azimuth becomes largely irrelevant. In practice, a zero-tilt configuration is uncommon due to increased dirt accumulation, prolonged snow coverage, and water drainage issues. But in terms of annual energy yield, PV panels mounted horizontally achieve approximately 85–90 % of the output of the ideal configuration, which corresponds to south-facing panels with a tilt angle of 30–35°. By contrast, north-facing panels with a typical tilt receive only 55–65 % of the ideal yield, representing a worst-case scenario. Although the zero-tilt assumption does not represent the optimal installation, it provides a realistic approximation of various suboptimal mounting conditions encountered in practice.

$$\boldsymbol{J_S = f(t)} \tag{1}$$

Function f defines received solar radiation J_S as a function of time during the year (day of year and time of day) and is implemented as a look-up table, obtained from publicly available data [38]. Fig. 3 shows the time profile of solar radiation through the year. Based on solar radiation J_S, power plant area A and efficiency μ, the generated electric power P_{PV} is determined:

$$P_{PV} = J_S \bullet A \bullet \mu \tag{2}$$

3.2. Electric energy consumption model

Electric energy consumption in residential buildings is attributed to various sources such as heating (via a heat pump), air conditioning, ventilation, lighting, kitchen appliances, entertainment systems, and similar devices. Generally, the daily time profile of electric consumption depends on the season (summer or winter), the type of day (working day, weekend, or holiday), and the personal habits of the residents. The

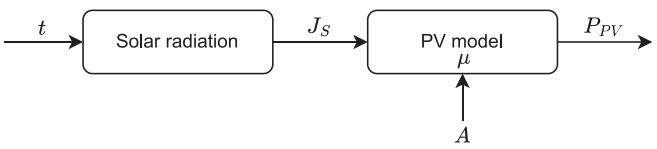

Fig. 2. PV model: relationship between time (t) and generated electric power (P_{PV}).

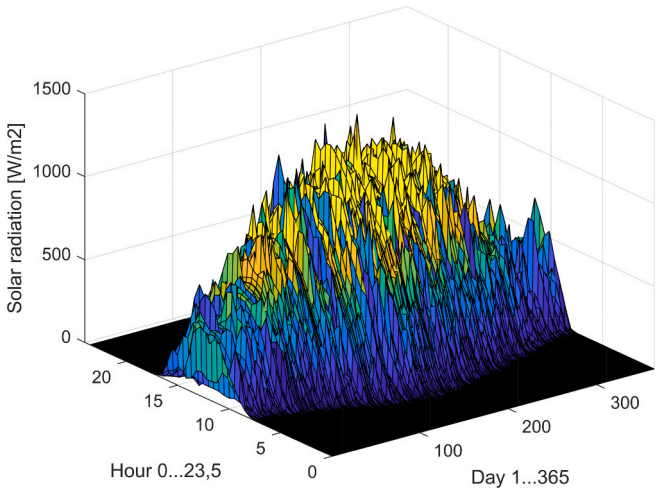

Fig. 3. Solar radiation as a function of time of year.

model represents the relationship between the time of year and consumed electric power (P_C), as shown in Fig. 4.

The model represents historical data on the consumption of a typical residential building and was obtained from the open data source HEAPO [39]. The data was collected in the canton of Zurich, Switzerland. It is organised as a yearly look-up table (time vs consumed electric power in 15-minute intervals) and is shown in Fig. 5 and Fig. 6. The yearly time profile data is disaggregated into two categories: 1. all appliances except the heat pump, and 2. the heat pump. The distinction is logical, as the heat pump is a significant consumer and its consumption can be reduced by utilising the dissipated heat from the fuel cell.

The reference building from the HEAPO dataset has a living area of 220 m^2 and three occupants. As shown in Fig. 5 and Fig. 6, the annual electricity consumption of household loads (excluding the heat pump) is 5712 kWh, while the heat pump accounts for an additional 6310 kWh. This results in a total annual electricity demand of 12,022 kWh.

Alternative data sources and standards are also available. For example, the VDI 4655 standard, applied in [54], assumes a well-insulated residential building with a living area of 160 m^2 and annual electricity consumption of 2350 kWh for household loads and 4000 kWh for the heat pump. These values are significantly lower than those obtained in the present study. The differences can be attributed to variations in building size, insulation level, climatic conditions, number and type of appliances, and occupant behaviour.

3.3. Electrolyser model

A simple electrolyser model is used, describing its relevant properties, particularly energy efficiency and operational power limitation. Although the electrolyser is a dynamic system, a static approximation is applied, representing the relationship between input electric power P_{EL_E} and the mass flow of the generated hydrogen ϕ_{H2}, as shown in Fig. 7.

Proton exchange membrane (PEM) electrolysers and fuel cells are known for their rapid response to changes in load demand. The load can be changed from minimum to maximum within a few seconds [48,50], which is significantly shorter than the 30-minute simulation step used in this study. Therefore, static models can be used without compromising simulation accuracy.

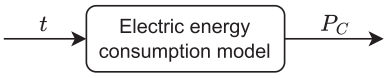

Fig. 4. Electric consumption model: relation between time (t) and consumed power (P_C).

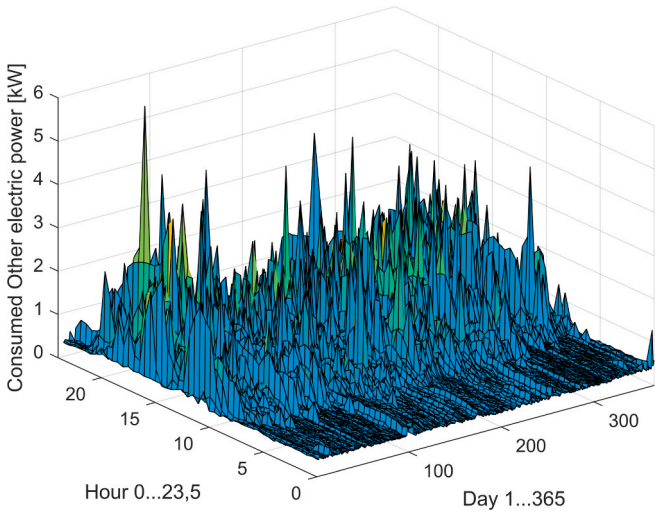

Fig. 5. Electricity consumption of appliances (excluding heat pump) as a function of time of year.

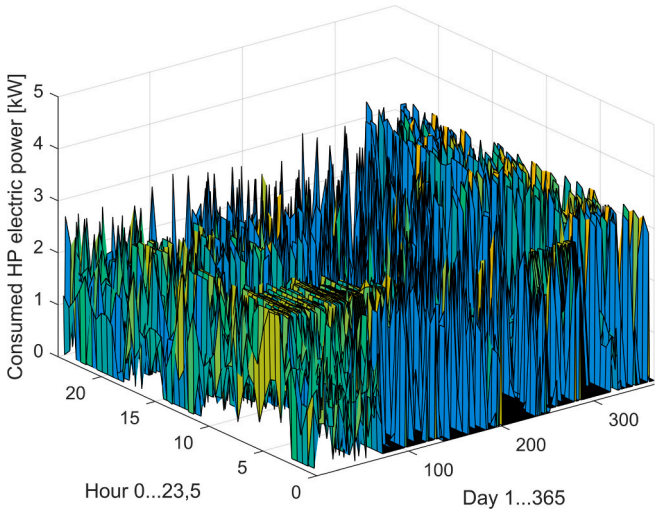

Fig. 6. Electricity consumption of the heat pump as a function of time of year.

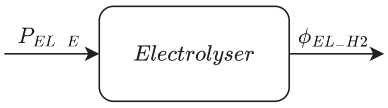

Fig. 7. Electrolyser model.

The output power of the generated hydrogen is determined by its mass flow rate and the heating value of hydrogen:

$$P_{EL\_H2} = \phi_{EL\_H2} \bullet HHV \tag{3}$$

Energy efficiency can be defined as the ratio of the output power of the generated hydrogen, P_{EL_H2}, to the input electric power to the electrolyser, P_{EL_E}:

$$\eta_{EL} = \frac{P_{EL\_H2}}{P_{EL\_E}} \tag{4}$$

The difference between the input electric power and the output hydrogen power represents thermal losses:

$$P_{EL\_T} = P_{EL\_E} - P_{EL_{H2}} = P_{EL\_E}(1 - \eta_{EL}) \tag{5}$$

Fig. 8 shows the typical relationship between input and output power, as well as the relation between input power and efficiency. The data in the figure are from a commercially available electrolyser.

The turn-down ratio of the electrolyser is assumed to be 10 %, as confirmed by several manufacturer specifications and the literature, e.g. [45]. This means that operation below 10 % of the nominal (maximum) electric power is generally not possible.

In general, energy efficiency decreases as operating power increases due to greater ohmic and mass transport losses. However, efficiency is also somewhat lower at very low operating power, because the electrolyser's balance of plant components consume electric power even at low loads. As the nominal power of the electrolyser may change and be optimised, the power in Fig. 8 is expressed in relative units (0…1). Engineering units (kW) are obtained by multiplying the relative units by the nominal electric power of the electrolyser.

Electrochemical systems (electrolysers, fuel cells, batteries) degrade over time due to ageing, use, and specific operating conditions (such as repeated start-up and shut-down events, and rapid load changes). For electrolysers and fuel cells, the degradation leads to reduced efficiency. Generalised and reliable degradation models are difficult to obtain, as they depend on the specific device type. In this study, it is assumed that electrolyser efficiency decreases proportionally with age by 1 % per year (for example, if the nominal efficiency is 70 %, after one year, it drops to 70 % × 99 % = 69,3 % and after ten years to 70 % × 90 % = 63 %). This assumption is supported by literature data [52] for electrolysers and [53] for fuel cells. Fig. 8 shows two curves for both efficiency and output hydrogen power: a new system, and a ten-year old system. In the simulation study, a ten-year old system is assumed, representing the worst case scenario. It is assumed that after ten years of operation, the electrolyser is retrofitted with new electrochemical cells to achieve a total lifespan of twenty years. A ten-year expected lifespan for electrolysers and fuel cells is realistic and supported by the literature, e.g. [51].

3.4. Fuel cell model

The fuel cell converts stored hydrogen and oxygen from ambient air into electric energy and water, which is reverse process of to the electrolyser. The model defines the relationship between the input hydrogen mass flow and the output electric power, which then determines the efficiency (Fig. 9). The relationship between these two variables is nonlinear, as the efficiency of the fuel cell decreases with load, that is, with operating power.

As with the electrolyser, a simplified model is used. In general, efficiency is defined as the ratio of the output electric power of the fuel cell

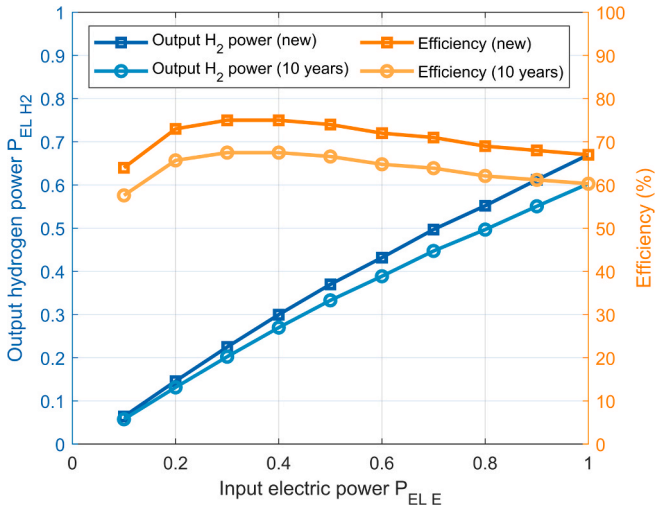

Fig. 8. Electrolyser output power and efficiency as functions of input power.

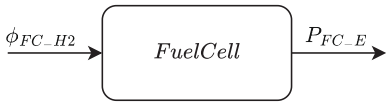

Fig. 9. Fuel cell model.

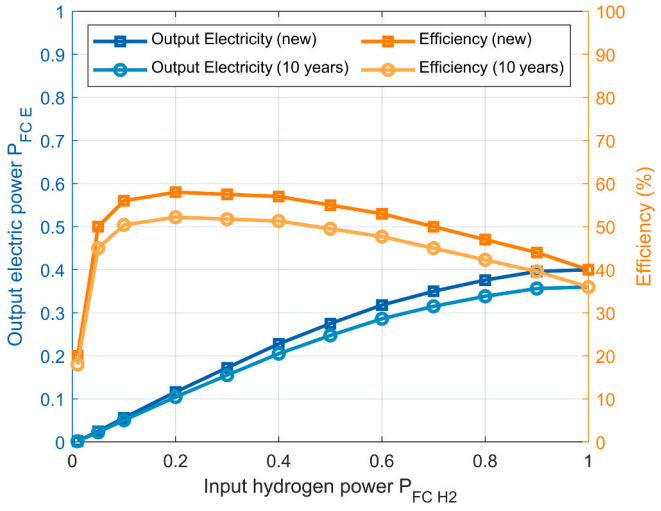

Fig. 10. Fuel cell efficiency and output power as functions of input power.

to the power of the consumed hydrogen:

$$\eta_{FC} = \frac{P_{FC\_E}}{P_{FC\_H2}} \tag{6}$$

The input power of the consumed hydrogen is determined by its mass flow rate and the heating value of hydrogen:

$$P_{FC\_H2} = \phi_{FC\_H2} \bullet HHV \tag{7}$$

Based on this, the fuel cell output electric power (P_{FC_E}) and thermal losses (P_{FC_T}) can be expressed as follows:

$$P_{FC\_E} = P_{FC\_H2} \bullet \eta_{FC} = \phi_{FC\_H2} \bullet HHV \bullet \eta_{FC} \tag{8}$$

$$P_{FC\_T} = P_{FC\_H2} \bullet (1 - \eta_{FC}) = \phi_{FC\_H2} \bullet HHV \bullet (1 - \eta_{FC}) \tag{9}$$

The fuel cell is also subject to degradation. The same assumptions regarding degradation, lifetime, and retrofitting are used as for the electrolyser.

3.5. Hydrogen storage model

Hydrogen is stored in a pressurised tank. The input flow rate is produced by the electrolyser, while the output flow rate is determined by the fuel cell (Fig. 11). Mathematically, the hydrogen storage tank acts as a time integrator of the difference between the thermal power of the hydrogen generated by the electrolyser P_{EL_H2} and the thermal power of the hydrogen consumed by the fuel cell P_{FC_H2}.

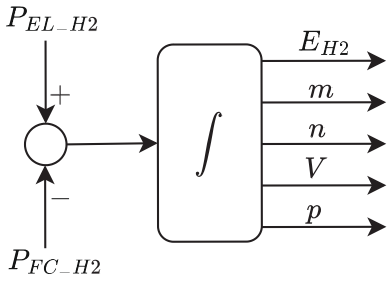

Fig. 11. Hydrogen storage model.

$$E_{H2} = E_{H2\_INIT} + \int_0^t (P_{EL\_H2} - P_{FC\_H2})dt \tag{10}$$

The amount of hydrogen in the tank can generally be expressed in several equivalent ways: as a mass m (kg), an amount n (mol), or an energy E (kWh). The relationships between these variables are well-known and defined by static algebraic equations. The relationship between m and n is given by the molar mass of hydrogen M.

$$m = M \bullet n \tag{11}$$

The energy of hydrogen in the tank is proportional to the mass of hydrogen, m,and its higher heating value, HHV.

$$E = m \bullet HHV \tag{12}$$

The pressure in the tank is proportional to the mass m of stored hydrogen and can be expressed by the ideal gas equation:

$$p = \frac{n \bullet R \bullet T}{V_T} = \frac{m \bullet R \bullet T}{M \bullet V_T} \tag{13}$$

In the equation above, V_T represents the geometric volume of the storage tank. The amount of hydrogen V in normal cubic metres (Nm^3) is also given by the general gas law, considering standard conditions (T = 273 K, p = 100000 Pa):

$$V = \frac{n \bullet R \bullet T}{p} \tag{14}$$

The storage capacity of the hydrogen tank is determined by its geometric volume V_T and the maximum pressure p_{MAX}:

$$E_{H2\_MAX} = \frac{p_{MAX} \bullet M \bullet V_T}{R \bullet T} \bullet HHV \tag{15}$$

E_{H2_MAX} represents the maximum amount of hydrogen thermal energy that can be stored in the tank. To prevent excessive charging or discharging, two status signals, T_F and T_E, indicate 'tank full' and 'tank empty' conditions respectively ($T_F = 1$ if $E_{H2} > 0.98\, E_{H2\_MAX}$) and ($T_E = 1$ if $E_{H2} < 0.02\, E_{H2\_MIN}$).

3.6. Battery model

Similar to the hydrogen storage tank, the battery is also modelled as an integrator of the difference between input and output electric power. Input power represents battery charging, while output power represents discharging. The battery model also accounts for losses during charging and discharging, which occur in the battery and its power electronic circuits (DC/DC converters). The model is shown in Fig. 12.

During charging, electric power P_{B_IN} flows into the battery, but not all of it is used for charging due to losses. The reduced power $P_{B\_IN\_C}$ represents the useful charging power, which is subject to integration. The relationship between the two is defined by the charging efficiency η_C, which is typically around 95 %.

$$P_{B\_IN\_C} = P_{B\_IN} \bullet \eta_C \tag{16}$$

A similar situation occurs during discharging; the output power $P_{B\_OUT\_D}$ flowing from the battery is also subject to losses, and the reduced value P_{B_OUT} is the power actually available to consumers. The relation between the two is determined by the discharging efficiency η_D, which is typically also around 95 %.

$$P_{B\_OUT} = P_{B\_OUT\_D} \bullet \eta_D \tag{17}$$

Finally, the battery state of charge is determined by integrating the input and output power over time:

$$E_B = E_{B\_init} + \int_0^t (P_{B\_IN\_C} - P_{B\_OUT\_D})dt \quad (18)$$

E_{B_MAX} represents the capacity, i.e. the maximum amount of energy that can be stored in the battery. To prevent excessive charging or discharging, two status signals B_F and B_E are provided to indicate 'battery full' and 'battery empty' events: ($B_F = 1$ if $E_B > 0.98\ E_{B\_MAX}$) and ($B_E = 1$ if $E_B < 0.02\ E_{B\_MIN}$).

Battery performance degrades with calendar ageing and cycling, resulting in reduced usable capacity and reduced charge and discharge efficiency. According to literature data [46], lithium-ion batteries of the $LiFePO_4$ (LFP) type used for daily energy balancing can sustain more than 4000 cycles at 80 % depth of discharge (DoD), with a typical capacity loss of 20–30 %. This cycle life is sufficient for approximately 10 years of daily operation, after which battery replacement is required. The simulation is conducted for a worst-case scenario, assuming a battery at the end of its 10-year lifetime. The nominal battery capacity ($E_{B\_MAX\_N}$) is calculated as:

$$E_{B\_MAX\_N} = \frac{E_{B\_MAX\_R}}{DoD \bullet 75\%} \quad (19)$$

where 75 % represents the expected remaining capacity after 10 years of operation. The required capacity ($E_{B\_MAX\_R}$) is the capacity actually needed to perform daily energy balancing. The nominal battery capacity, $E_{B\_MAX\_N}$, is used for CAPEX calculation.

For charging and discharging efficiencies, it is assumed they decrease from the original 97 % to 95 % over ten years. This results in a round-trip efficiency drop from 95 % to 90 %. This is, in fact, a pesimistic estimate, as [47] indicates that after 2500 cycles the round-trip efficiency remains above 94 %.

In reality, battery efficiency also depends on temperature, but this effect is not significant, as it is assumed the battery is installed inside the building at a relatively stable temperature. The dependence of efficiency on charge and discharge rates is also not modelled, as these rates are actively controlled and limited by the power management algorithm described later.

$$\begin{aligned} e < e_{min} &\rightarrow P_{HP\_T\_DEM} = 0 \\ e_{min} \le e \le e_{max} &\rightarrow P_{HP\_T\_DEM} = P_{HP\_T\_min} + (P_{HP\_T\_max} - P_{HP\_T\_min}) \bullet \frac{e - e_{min}}{e_{max} - e_{min}} \\ e > e_{max} &\rightarrow P_{HP\_T\_DEM} = P_{HP\_T\_max} \end{aligned} \quad (21)$$

3.7. Fuel cell and heat pump thermal integration

As shown in the fuel cell efficiency diagram (Fig. 10), the fuel cell generates significant losses (40 % or more) as heat, which must be removed by the cooling circuit. The temperature of the cooling medium is around 80°C for LT-PEM and around 200°C for HT-PEM fuel cells, meaning the generated heat can be relatively easily used for building and sanitary water heating [40]. In this way, the load on the heat pump can be reduced, resulting in savings of electric energy and hydrogen.

The utilization of fuel cell waste heat is well established and has been widely implemented in combined heat and power (CHP) systems, as documented in the literature. However, specific heat utilization concepts differ in their implementation and control strategy.

If fuel cell waste heat is used directly and no thermal storage is available, the system typically operates in heat-led operation. In this case, the fuel cell output is driven by thermal demand, while electricity is generated as a by-product that can be either consumed locally or exported to the grid. An example of this approach is reported in [56]. Conversely, in electricity-led operation, the fuel cell follows electrical demand. Thermal energy is generated as a by-product and can be utilized to satisfy local thermal demand; however, if the available heat exceeds demand, the surplus must be rejected.

A key challenge in both approaches is the temporal mismatch between electricity and heat demand, which can result in surplus electricity or excess thermal energy. To address this issue, a thermal energy storage (buffer) is introduced in the present study. The heat storage decouples thermal and electrical demand, enabling electricity-led operation while storing excess heat for later use.

The situation is illustrated in Fig. 13, where the blocks FC, HP, and CONS represent the fuel cell, the heat pump, and other electric consumers, respectively. P_{FC_T} represents fuel cell thermal losses. It is assumed that 60 % of the fuel cell thermal losses can be utilised. To study its effect in simulation experiments, thermal integration can be switched on or off by directing the heat stream P_{FC_T} to the heat storage or to the ambient (not utilising it).

To continuously balance heat generation and consumption, a liquid-based heat storage system is assumed, which stores heat generated by the heat pump and heat from the fuel cell cooling circuit. Heat storage is a common component in heat pump systems. Heat generation and consumption are balanced by maintaining an approximately constant thermal energy content in the storage. In practice, the thermal energy content is estimated by measuring the temperature of the liquid, taking into account its mass and thermal capacity. For control, a simple proportional control law is used, which considers the power limitations of the heat pump. The currently demanded thermal power of the heat pump ($P_{HP\_T\_DEM}$) is determined by the control error, i.e. the difference between the setpoint (E_{ST_SET}) and the actual energy content in the storage (E_{ST_ACT}):

$$e = E_{ST\_SET} - E_{ST\_ACT} \quad (20)$$

The control law is given by the equation below and illustrated in Fig. 14. $P_{HP\_T\_max}$ and $P_{HP\_T\_min}$ denote the maximum and minimum thermal power of the heat pump, respectively. The parameters e_{min} and e_{max} determine the slope (the proportional gain) of the linear section of the control law.

During the experiments, the following parameters were used: E_{ST_SET} = 70 kWh, e_{min} = 4 kWh, e_{max} = 20 kWh, $P_{HP\_T\_max}$ = 12 kW, $P_{HP\_T\_min}$ = 2.4 kW (20 % turn-down ratio). The results are presented in the Simulation study section.

3.8. Economic model

The economic model estimates the resulting price of the supply of electric energy (*EP*) to the electric consumers of the building over a one-year period. This can then be compared to the price of the supply from the public electric grid. For the analysis, the price of the local energy supply is broken down into components incurred by specific elements of the system. The price components EP_{PV}, EP_{BATT}, EP_{EL}, EP_{FC}, and EP_{H2_STOR} are incurred by the PV power plant, battery, electrolyser, fuel cell and hydrogen storage, respectively. Each price component is calculated by dividing the capital expenditure of the element ($CAPEX_X$) by the lifetime of the element t_{L_X}, as the cost is evenly distributed over the

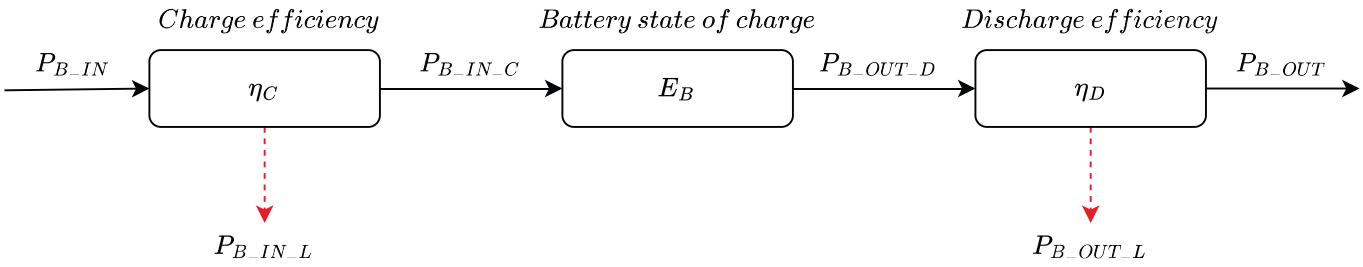

Fig. 12. Battery model.

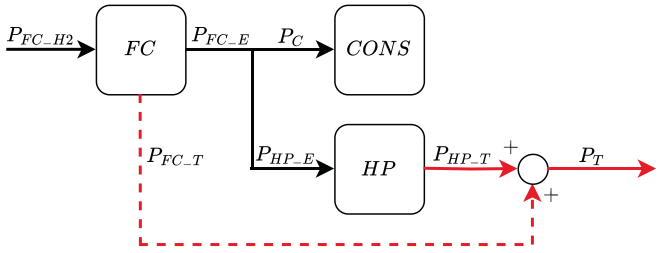

Fig. 13. Thermal integration of fuel cell and heat pump.

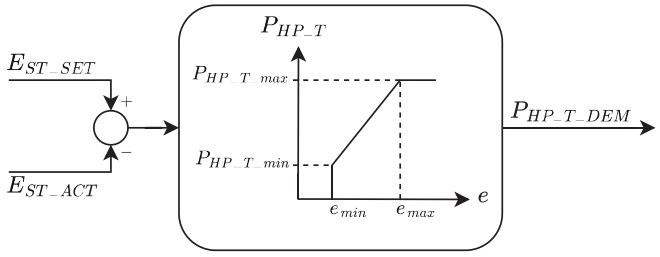

Fig. 14. Heat storage control law.

Table 2
Cost of the supply from the public electric grid (Germany).

Energy and supply costs (EUR/kWh)	Network costs (EUR/kWh)	Taxes, fees, levies and charges (EUR/kWh)	Total price (EUR/kWh)
0.1640	0.0909	0.1064	0.3613

entire lifetime. The same form of the equation is used for all price components (X = PV, BATT, EL, FC, H2_STOR).

$$EP_X = \frac{CAPEX_X}{t_{L\_X}} \tag{22}$$

Based on manufacturers' data and information from the literature, the relative costs of the elements are given in Table 3 and Table 4 (System economic parameters). Actual costs are calculated by multiplying the relative costs of the elements by their assumed capacities or sizes. The expected lifetime (t_{L_X}) of a particular element depends on many factors, but for simplicity, it is assumed that the lifetime of each element is 20 years. This is a very rough estimate; actual degradation progresses with ageing, usage intensity, and mode of operation (e.g. frequent start/stop of the electrolyser and the fuel cell increases their degradation). In this study, degradation of electrochemical components (electrolyser, fuel cell, battery) is considered in a simplified manner. For the electrolyser and fuel cell, a drop in efficiency is assumed, as explained in sections 3.3 and 3.4. It is assumed that both components must be retrofitted with new electrochemical cells after 10 years to achieve 20 years of operation. Retrofit costs are included in operational expenditures (OPEX), which are assumed to be 3 % of CAPEX each year – in 20 years, this amounts to 60 % of CAPEX. Battery degradation is reflected in reduced capacitiy and efficiency, as explained in section 3.6. The nominal capacity of a new battery is used for CAPEX calculation, while the remaining capacity after 10 years is used for energy balance simulations. Replacement of the battery after 10 years is considered.

To compare the costs of the proposed local energy supply with those of the public electric grid, data from Eurostat's dataset (Electricity price components for household consumers – annual data) [41] was used. Data for Germany in 2024, covering the consumption range from 5 to 14,999 kWh/year, was considered. The relevant cost components are summarised in Table 2.

4. Power management

A control strategy is required to balance electric energy generation and consumption through battery charging/discharging and hydrogen generation/utilization. The presence of two energy storage devices (the battery and hydrogen system) offers various control options and increases the complexity of the control algorithm. In this study, a simple yet effective control algorithm was developed. The main idea is to use the battery for daily balancing as its round-trip efficiency is much higher than that of the hydrogen system. For seasonal balancing (storing excess power generated in summer for use in winter), the hydrogen system is employed. This means the battery is given priority over the hydrogen system for balancing actions. This is achieved with the following control algorithm. When the generated PV power exceeds the consumed power, the excess power (P_E) is directed to the battery considering the maximum charging power and available free capacity. Any power that cannot be stored in the battery is then supplied to the electrolyser to be converted into hydrogen, considering the electrolyser's minimum and maximum power limits and the available capacity in the hydrogen tank. If the battery and electrolyser cannot absorb all the excess power, the remaining surplus is exported to the grid. The corresponding control diagram is shown in Fig. 15.

In the opposite case, when the generated PV power is lower than the consumed power, the missing power (P_E, negative in this case) is supplied by the battery, considering the maximum discharging power and the available energy in the battery. If the battery cannot supply all the missing power, the reminder is provided by the fuel cell, which converts stored hydrogen into electric power. The maximum electric power of the fuel cell and the available hydrogen in the tank are considered. If the battery and fuel cell together cannot provide all the missing power, the reminder is drawn from the grid. One of the design goals is to eliminate or minimise the amount of electric energy taken from the grid. The corresponding control diagram for this case is shown in Fig. 16. The proposed power management algorithm (Fig. 15, Fig. 16) can be directly implemented using block-oriented simulation tools (e.g. MATLAB Simulink) or by programme code (MATLAB script), the latter being available in the Supplementary material.

Table 3
System parameters and results of experiments 1…9.

System structure		Experiment								
		1	2	3	4	5	6	7	8	9
FC-HP thermal integration	No/Yes	No	No	No	Yes	Yes	Yes	Yes	Yes	Yes
Battery	No/Yes	No	No	Yes	No	Yes	Yes	Yes	No	No
Technic parameters										
PV size	m^2	147.7	149.3	108.1	129.9	109.2	111.2	98.4	128	128.7
Hydrogen storage tank	kWh	6914.8	6926.1	6632.3	6157.2	6058.2	5945.8	5717.0	6190.6	6147.2
capacity	kg	175.5	175.8	168.4	156.3	153.8	150.9	145.1	157.2	156.1
Electrolyser max. power	kW	13	13	13	13	13	11	10	14	13
Electrolyser min. power	% of max P	0 %	10 %							
Electrolyser efficiency	%	See Figure 8 (10 years)								
Fuel cell max. power	kW	13	13	13	13	13	10	10	12	12
Fuel cell efficiency	%	See Figure 10 (10 years)								
Battery required capacity	kWh	0		16	0	7	6	20	0	
Battery nominal capacity	kWh	0		26.7	0	11.7	10	33.3	0	
Batt. max. charging power	kW	0		8	0	8	8	8	0	
Batt. max. discharg. power	kW	0		8	0	8	8	8	0	
Battery charging efficiency	%	n.a.		95%	n.a.	95%			n.a.	
Battery discharging effic.	%	n.a.		95%	n.a.	95%			n.a.	
Economic parameters										
PV power plant *CAPEX*	EUR/m^2	210								
Electrolyser *CAPEX + OPEX*	EUR/kW	800+480								
Fuel cell *CAPEX + OPEX*	EUR/kW	800+480								
H2 storage tank *CAPEX*	EUR/kg	250								
Battery *CAPEX + OPEX*	EUR/kWh	400+400								
Results: operating time										
Electrolyser total	h	3473.5	2932	1757.5	2826	2044	2080.5	1649.5	2763.5	2812.5
Electrolyser effective	h	1661.4	1652.3	893.5	1444.9	1014.6	1144.2	973.4	1319.9	1428.3
Fuel cell total	h	5286	5280	2253.5	5314	3123.5	3447.5	2135.5	5331.5	5326.5
Electrolyser effective	h	499.4	498.7	288.3	429.5	319	447.9	312.2	467.8	467.5
Results: energy balance										
PV generated energy	kWh	27835.3	28136.8	20372.3	24480.7	20579.6	20956.6	18544.3	24122.7	24254.6
Consumed energy	kWh	12022.2	12022.2	12022.2	10747.3	11152	11156.9	11415.5	10777.4	10778.3
Energy supplied to the grid	kWh	707.4	1118	152.3	534	179.8	278.8	166.3	481.1	517.9
Energy taken from the grid	kWh	0	0	0	0	0	0	0	0	0
Electrolyser losses	kWh	8030.1	7928.9	4132.3	6817.9	4680.5	5004.7	3571.8	6618.8	6730
Fuel cell losses	kWh	7069.3	7058.9	3724.5	6377.9	4353.9	4329.6	3035.2	6227.7	6223
Battery charging losses	kWh	0	0	168.8	0	104.5	93.5	179.1	0	0
Battery discharging losses	kWh	0	0	160.3	0	99.3	88.8	170.1	0	0
Hydrogen produced	kg	344.5	344	190	303.8	216	220.1	156.4	301.1	300.5
Results: price of electric energy (by components and total)										
EP_{PV}	EUR/MWh	129	130.4	94.4	126.9	102.8	104.7	90.5	124.7	125.4
EP_{H2_STOR}	EUR/MWh	182.5	182.8	175.1	181.8	172.4	169.1	158.9	182.3	181
EP_{EL}	EUR/MWh	69.2	69.2	69.2	77.4	74.6	63.1	56.1	83.1	77.2
EP_{FC}	EUR/MWh	69.2	69.2	69.2	77.4	74.6	57.4	56.1	71.3	71.3
EP_{BATT}	EUR/MWh	0	0	88.7	0	41.8	35.9	116.8	0	0
EP_{TOT}	EUR/MWh	449.9	451.6	496.6	463.5	466.3	430.1	478.4	461.4	454.8
Results: Annual cost of local supply										
Consumed el. energy	kWh	12022.2	12022.2	12022.2	10747.3	11152	11156.9	11415.5	10777.4	10778.3
Final price	EUR/MWh	449.9	451.6	496.6	463.5	466.3	430.1	478.4	461.4	454.8
Total cost	EUR	5409.2	5429.6	5970.4	4981.9	5199.8	4798.4	5460.8	4972.5	4902.1
Results: Annual cost of traditional supply (from public electric grid)										
Consumed el. energy	kWh	12014								
Final price	EUR/MWh	361.3								
Total cost	EUR	4340.7								

5. Simulation study

The main purpose of the simulation study is to determine the combinations of system parameters (PV power plant size, battery capacity, electrolyser power, fuel cell power, and hydrogen storage capacity) that meet the electric energy demands of the building over one-year period. A further goal is to identify optimal parameter combinations that yield the best values for selected technical or economic key-performance indicators, particularly the annual cost of electric energy supply.

5.1. Initial component sizes

Before running the simulation experiments, it is necessary to determine the initial sizes of the system components.

Table 4
System parameters and results of experiments 10…18.

System structure		Experiment								
		10	11	12	13	14	15	16	17	18
FC-HP thermal integration	No/Yes	Yes	Yes	Yes	Yes	Yes	Yes	Yes	Yes	Yes
Battery	No/Yes	No	No	No	No	No	No	No	Yes	Yes
Technic parameters										
PV size	m^2	130.4	133.7	139	148.1	163.2	190	172.6	132.6	132.6
Hydrogen storage tank capacity	kWh	6083.2	5990.6	5835.7	5619.6	5335.5	4981.8	5128.8	5327.8	5327.8
	kg	154.4	152.1	148.2	142.7	135.5	126.5	130.2	135.3	135.3
Electrolyser max. power	kW	12	11	10	9	8	7	7	7	7
Electrolyser min. power	% of max P	10 %								
Electrolyser efficiency	%	See Figure 8 (10 years)								
Fuel cell max. power	kW	12	12	12	12	12	12	6.2	6.2	6.2
Fuel cell efficiency	%	See Figure 10 (10 years)								
Battery required capacity	kWh	0							6	6
Battery nominal capacity	kWh	0							10	10
Batt. max. charging power	kW	0							8	8
Batt. max. discharg. power	kW	0							8	8
Battery charging efficiency	%	n.a.							95 %	
Battery discharging effic.	%	n.a.							95 %	
Economic parameters										
PV power plant *CAPEX*	EUR/m^2	210								
Electrolyser *CAPEX + OPEX*	EUR/kW	800+480								400+240
Fuel cell *CAPEX + OPEX*	EUR/kW	800+480								400+240
H2 storage tank *CAPEX*	EUR/kg	250								125
Battery *CAPEX + OPEX*	EUR/kWh	400+400								200+200
Results: operating time										
Electrolyser total	h	2870	2933	3115	3000.5	3232.5	3404.5	3325.5	2455	2455
Electrolyser effective	h	1555.0	1703.6	1875.9	2080.9	2327.1	2627.4	2511.2	1905.1	1905.1
Fuel cell total	h	5314	5299	5273.5	5233	5174.5	5085	5141.5	3230	3230
Electrolyser effective	h	466.6	465.1	462.9	459.2	453.8	445.7	886.5	675.9	675.9
Results: energy balance										
PV generated energy	kWh	24575	25196.9	26195.7	27910.7	30756.4	35807.1	32527.9	24989.6	24989.6
Consumed energy	kWh	10780.7	10784.2	10790.4	10800.1	10814.2	10835.4	10961.3	11221.9	11221.9
Energy supplied to the grid	kWh	733.5	1253.6	2201	3893.5	6770.9	11927.9	9484.9	4436.2	4436.2
Energy taken from the grid	kWh	0	0	0	0	0	0	0	0	0
Electrolyser losses	kWh	6844.9	6954	7037	7097.8	7125.1	7102.4	6770.1	5140	5140
Fuel cell losses	kWh	6211.2	6193.5	6162.6	6114	6043.6	5937.3	5307.6	4004.1	4004.1
Battery charging losses	kWh	0	0	0	0	0	0	0	95.5	95.5
Battery discharging losses	kWh	0	0	0	0	0	0	0	90.7	90.7
Hydrogen produced	kg	300	299.2	297.6	295.3	291.7	286.6	274.4	208.1	208.1
Results: price of electric energy (by components and total)										
EP_{PV}	EUR/MWh	127	130.2	135.3	144	158.5	184.1	165.3	124.1	124.1
EP_{H2_STOR}	EUR/MWh	179.1	176.3	171.6	165.1	156.6	145.9	148.5	150.7	75.3
EP_{EL}	EUR/MWh	71.2	65.3	59.3	53.3	47.3	41.3	40.9	39.9	20
EP_{FC}	EUR/MWh	71.2	71.2	71.2	71.1	71	70.9	36.2	35.4	17.7
EP_{BATT}	EUR/MWh	0	0	0	0	0	0	0	35.6	17.8
EP_{TOT}	EUR/MWh	448.5	443	437.4	433.6	433.4	442.2	390.9	385.7	254.9
Results: Annual cost of local supply										
Consumed el. energy	kWh	10780.7	10784.2	10790.4	10800.1	10814.2	10835.4	10961.3	11221.9	11221.9
Final price	EUR/MWh	448.5	443	437.4	433.6	433.4	442.2	390.9	385.7	254.9
Total cost	EUR	4835.6	4776.9	4719.4	4682.4	4686.8	4791.9	4284.7	4327.8	2860.1
Results: Annual cost of traditional supply (from public electric grid)										
Consumed el. energy	kWh	12014								
Final price	EUR/MWh	361.3								
Total cost	EUR	4340.7								

- To perform daily balancing mainly with the **battery**, its capacity must be approximately equal to the difference between the generated and consumed energy in one day, considering the day with the highest difference.
- The required capacity of the **hydrogen storage** tank is obtained from the simulation results: in the model, a significantly oversized capacity is assumed, and the actual required capacity is equal to the difference between the minimum and maximum amount of hydrogen in the storage tank over the course of the year.
- The **maximum discharging power of the battery** and the **maximum power of the fuel cell** are set to the maximum excess of power consumed over power generated.
- Similarly, the **maximum charging power of the battery** and the **maximum power of the electrolyser** are set to the maximum excess

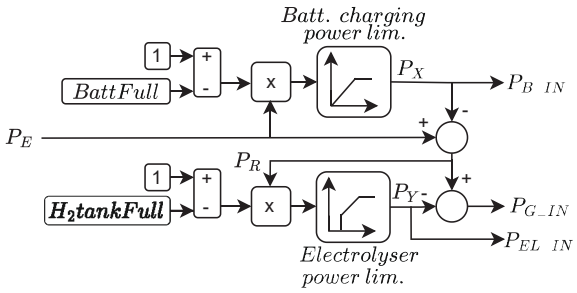

Fig. 15. Power management in the case of PV power excess.

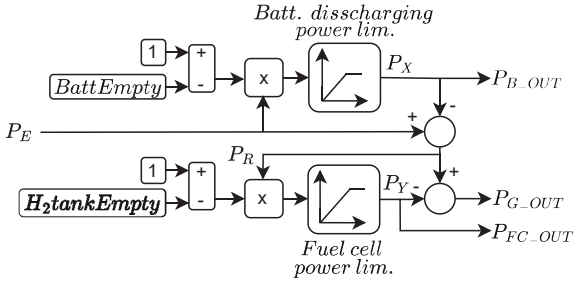

Fig. 16. Power management in the case of PV power deficit.

of power generated over power consumed. In this way, the battery and the hydrogen system can independently compensate for the difference between generated and consumed power at any moment.

5.2. Simulation period

Significant energy fluctuations occur on daily and yearly cycles. Year-to-year fluctuations exist but are beyond the scope of this work. Therefore, the simulation scenarios start at the beginning of the year and cover a one-year period. The simulation time step is 30 min. For comparison, all simulation scenarios use the same solar radiation data (Section 3.1) and household consumption data (Section 3.2). At the start of the year, when PV power generation is low due to winter at the use-case location, stored hydrogen energy must be used. Thus, a sufficient amount of hydrogen must be available in the storage tank at the beginning of the year. Once consumed, the hydrogen must be regenerated during the summer to ensure that the stored hydrogen at the end of the year matches the initial amount.

5.3. Results

Fig. 17 shows an example of the complete system operation over one-year period. The system parameters for this example are listed in Table 3, column Experiment 7.

The plots in the top row show the stored energy (state of charge) in the hydrogen tank (left) and in the battery (right). In the hydrogen tank storage plot, a yearly cycle is clearly visible, with the solar deficit draining the tank in winter and the surplus refilling it in summer. In contrast, the dispersed fluctuations in the battery energy (state-of-charge) indicate that the battery is used only for daily balancing. Generally, there are almost no daily fluctuations in the hydrogen tank, meaning the hydrogen system is rarely involved in daily balancing, which aligns with the initial concept of using the battery for daily balancing. It is important that the amount of hydrogen in the tank at the end of the year matches that at the beginning, ensuring that the yearly energy balance is achieved.

The plots in the second row show the actual electric power of the electrolyser (H2 input power) and the fuel cell (H2 output power) on the left, and the battery charging (Batt input power) and discharging (Batt output power) on the right. At the beginning of the year (days 1…80, and occasionally later), the fuel cell operates, meaning the PV power deficit is covered by converting stored hydrogen into electric energy. In the next period (days 50…100), occasional surpluses of PV power occur, resulting in the conversion of electric energy into hydrogen and vice versa. This is not optimal for efficiency, as storing energy as hydrogen has a significantly lower round-trip efficiency than storing it in the battery. This could be improved by increasing the battery's capacity and power, but this would also increase its cost. In the following period (days 100…300), there is a constant daily surplus of PV power; daily balancing is performed by the battery, excess PV energy is converted to hydrogen, and during this period, hydrogen is almost never converted back to electricity (the fuel cell does not operate). In the winter period (days 301…365), a PV power deficit appears again and is covered by converting stored hydrogen into electricity via the fuel cell, while the electrolyser rarely operates during this period.

The plots in the third row show household Excess power (left) and Grid power (right). The average excess power is positive during summer and negative during winter, indicating a deficit. Input grid power (supply to the grid) occurs when the system cannot use or store the generated energy, mostly in summer, and output grid power (consumption from the grid) is zero throughout the entire year.

The plots in the fourth row show the generated PV power on the left and the consumed power on the right. The mismatch between energy consumption and PV production, which needs to be balanced, is clearly visible.

If the system is installed and commissioned during the winter, the hydrogen tank must be prefilled with enough hydrogen to cover the winter. The initial amount of hydrogen can be supplied externally or generated by the electrolyser using electricity from the grid, but this is required only once during the system's lifetime. However, if the system is installed and started during the summer, initial prefilling is not necessary, as the system provides the winter energy reserve from the surplus energy generated in the summer.

5.4. Sensitivity analysis

In the next step, a simulation-based sensitivity analysis was conducted to test different combinations of system parameters. Each experiment is defined by a set of technical and economic parameters. Importantly, technical parameters are always set so that the initial and final amounts of hydrogen in storage are approximately equal, ensuring energy balance is maintained and allowing the same operational scenario to be repeated in subsequent years. Results are presented as energy balance data and the structure of system costs. The results show the price of electric energy for the local supply. However, even more important is the total annual cost of the local supply and its comparison with the total annual cost of conventional supply from the public electric grid. Parameters and results are collected in Table 3 and Table 4 and discussed.

In the first test (Exp. 1) the hydrogen system without the battery is considered. The minimum power of the electrolyser is assumed to be 0 %, which is unrealistic, as electrolysers cannot operate below a minimum power defined by technological limitations. In this case, the hydrogen system is used for both daily and seasonal balancing resulting in high conversion losses (8030.1 kWh and 7069.3 kWh) for the electrolyser and the fuel cell, respectively. In Exp. 2 and subsequent experiments, the minimum electrolyser power is set to a realistic 10 % of the maximum power, which worsens the situation since it is not possible to capture all the excess PV power. If the excess power is less than the minimum electrolyser power, it cannot be captured and must either be left unexploited or fed to the electric grid. This leads to increased energy supplied to the grid (from 707.4 to 1118 kWh), and to compensate for this, the size of the PV power plant must be increased (from 147.7 to 149.3 m^2). In Exp. 3, a battery is added to the system to perform daily balancing. As a result, the total conversion losses of the electrolyser and the fuel cell are reduced by almost 48 %. But this leads to decreased sizes

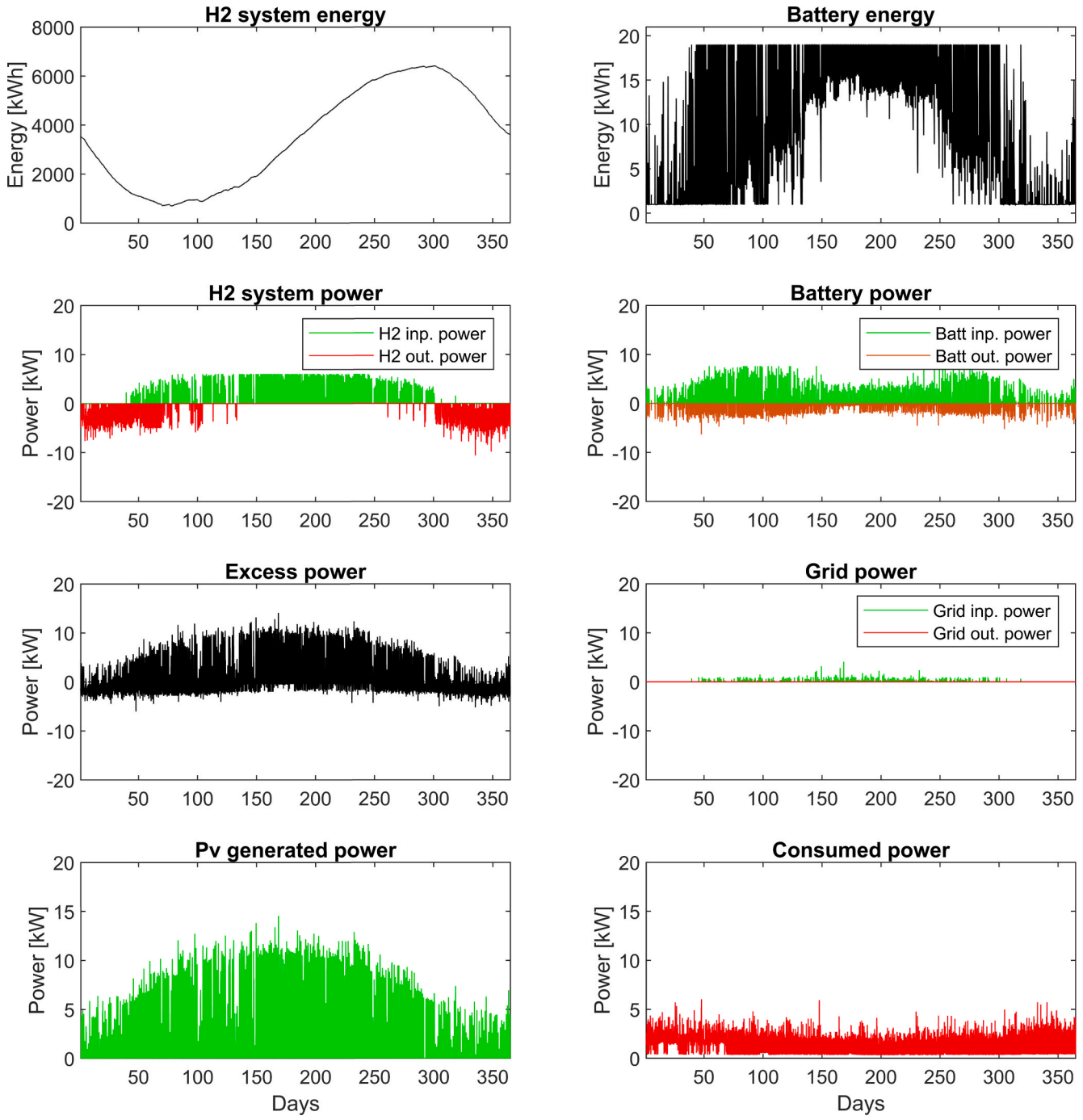

Fig. 17. An example of system operation during one-year period.

of the PV power plant (from 149.3 to 108.1 m^2) and the hydrogen storage tank (from 175.8 to 168.4 kg), resulting in higher system CAPEX and annual cost of electric energy supply. In Exp. 4, thermal integration of the heat pump and the fuel cell is introduced and the battery is removed. Thanks to thermal integration, annual electric energy consumption is reduced by 10 %, but conversion losses increase since there is no battery and the hydrogen system is also used for daily balancing. Utilising electrolyser losses also has potential benefits, but this was not studied. In Exp. 5, the battery is reintroduced to the system, resulting in significantly decreased conversion losses. To further optimise the system (Exp. 6), the maximum power of the electrolyser and fuel cell is decreased to 11 and 10 kW, respectively. However, this requires a slightly larger (+2 %) PV power plant but results in decreased costs of annual electric energy supply. In Exp. 7, the electrolyser maximum power is decreased to 10 kW and the battery capacity is increased to 20 kWh, which further decreases conversion losses but increases the total annual cost of supply (from 4798.4 to 5460.4 EUR).

In Exp. 8…16, the system without the battery was investigated again. This system appears attractive as it contains fewer components and is easier to operate and control. However, it inevitably results in significantly higher losses of electric energy due to the daily conversion of electric energy into hydrogen and vice-versa. Removing the battery has several opposing and competing effects on costs. The absence of the battery reduces the system's CAPEX, but the hydrogen subsystem must then perform both daily and seasonal energy balancing, which lowers overall storage efficiency due to the lower round-trip efficiency of the

hydrogen system compared to the battery. Additionally, it is not possible to capture excess PV power below the minimum operating threshold of the electrolyser (P_{EL_MIN}). To compensate for this, a larger PV system is required, which increases CAPEX and partially offsets the savings from battery elimination. On the other hand, the absence of the battery increases total fuel cell thermal losses, but utilising these losses reduces the load and electricity consumption of the heat pump. Fig. 21 and Fig. 22 show the percentage of the total heat demand covered by fuel cell losses (P_{FC_T}) throughout the year. Fig. 21 shows the case without the battery (Exp. 16), and Fig. 22 shows the case with the battery (Exp. 17). Since thermal losses of the fuel cell are higher without the battery, the contribution of fuel cell thermal losses to the total heat demand is also higher. The percentage is particularly higher in the summer period (days 180…250, i.e. July and August), when the total heat demand is lower and therefore fuel cell losses represent a higher percentage.

During Experiments 8…15, all parameters were kept constant except for the electrolyser maximum power, which was reduced from 14 to 7 kW in 1 kW increments. At each step, the PV power plant size was adjusted (increased) to ensure the yearly hydrogen balance (an equal amount of hydrogen in the tank at the beginning and end of the year). The results show that the minimum annual cost of electric energy supply is achieved with an electrolyser power of 7 kW, although the cost is not significantly lower than the average cost observed in experiments 8…15. A 7 kW electrolyser requires the smallest hydrogen storage tank (126.5 kg), which helps to reduce its physical size. The experiments demonstrate that a reduced electrolyser size and price must be offset by an increased size and cost of the PV power plant.

In Exp. 16, the fuel cell nominal power was reduced to 6.2 kW, the minimum power required to ensure that no energy was drawn from the grid. This further reduced the annual cost of electric energy supply to 4284.7 EUR.

Finally, in Exp. 17, the battery was reinserted to further improve the energy balance, but the resulting annual cost of electric energy increased slightly (4327.8 EUR).

To further reduce costs (Exp. 18), a 50 % subsidy for the CAPEX of the hydrogen system and the battery was assumed, which lowers the annual cost of electric energy supply to 2860.1 EUR.

The simulation is based on the current CAPEX and OPEX of the technological equipment, as shown in Table 3 and Table 4. The simulation does not assume any future CAPEX reductions or subsidies (except for Experiment 18). The results indicate that approximately the same annual cost of electric energy supply (about 4300 EUR) can be achieved with systems both without and with the battery (Exp. 16 and 17). This cost could be competitive with the annual expenditure for electric energy supplied from the public grid, but only in markets with high prices, such as Germany, where retail electricity prices are among the highest in Europe and annual cost reach 4341 EUR.

However, relative competitiveness may decrease when compared with electricity prices in other European countries. These findings indicate that the proposed local energy supply systems could be economically viable. However, this conclusion relies on assumed capital costs for the technological components, which remain uncertain due to limited manufacturer data. The greatest technical and economic challenge is compressed hydrogen storage. A storage capacity of approximately 130 kg is required to cover the deficit during the winter period. This results in large reservoir dimensions and structural challenges that increase with storage pressure. A reduction in hydrogen storage cost would have the greatest impact on lowering the annual cost of generated electricity.

The optimal configuration identified in Experiment 17 can be compared with similar system configurations reported in the literature. For example, the simulation study in [6] considers a setup with 21 kWp PV power plant (corresponding to approximately 130 m^2 of installed modules), combined with 10–20 kWh of battery storage, a 4 kW fuel cell, a 7 kW electrolyzer, and 170–190 kg of hydrogen storage. This system is designed for off-grid operation of a residential building in Finland with a living area of 183 m^2, covering both space heating and domestic hot water demand. This is consistent with the findings of Experiment 17. It should, however, be noted that the Finnish case study exhibits higher overall energy consumption at a comparable PV capacity. Consequently, a larger fraction of the summer PV surplus must be seasonally stored to cover winter demand, which leads to increased required capacities for both the battery system and the hydrogen storage tank.

Table 5
Annual electricity supply cost sensitivity to key CAPEX variations.

Component	CAPEX variation	Annual electricity supply cost variation
PV power plant	± 20 %	± 7.3 %
Electrolyser	± 20 %	± 1.5 %
Fuel cell	± 20 %	± 1.3 %
Hydrogen storage	± 20 %	± 8.9 %
Battery	± 20 %	± 1.0 %

Table 5 shows how the resulting annual electricity supply cost changes when the CAPEX of individual components (PV power plant, electrolyser, fuel cell, hydrogen storage, and battery) is varied by ± 20 %. The calculation is based on the system setup from Experiment 17. A reduction in hydrogen storage cost would have the greatest impact on lowering the annual cost of generated electricity.

Table 3 and Table 4 also show the annual operating times of the electrolyser and the fuel cell. The total operating time is the cumulative duration during which the units are switched on, while the effective operating time accounts for partial loading and is calculated by time integrating the normalised load (0…1) over the one-year period. Based on the total operating time, the electrolyser utilisation factor across the experiments ranges from 18.8 % to 39.7 %, while the fuel cell utilisation factor ranges from 24.3 % to 60.8 %. These relatively low utilisation levels also contribute to higher annual electricity supply costs. This situation could be improved by modifying the power management algorithm and increasing battery capacity. If daily excess energy were first stored in the battery, it could then be gradually converted into hydrogen throughout the day by operating the electrolyser at a lower and more constant power level. This approach would allow a reduction in the electrolyser's nominal power and CAPEX while increasing its utilisation rate. A similar operational strategy could also be applied to the fuel cell.

Results from Table 3 and Table 4 are also presented in figures for easier comparison. Fig. 18 shows the annual electricity supply costs for each experiment, with a breakdown of contributions from individual

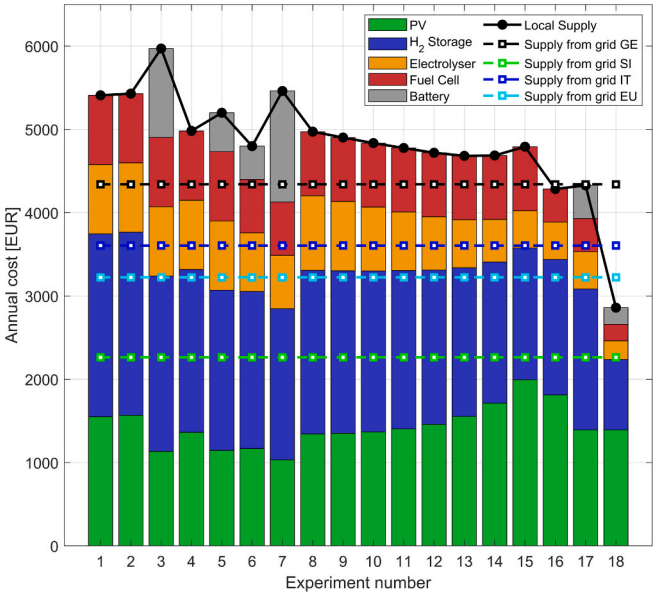

Fig. 18. Components of the annual cost of electricity and heat supply.

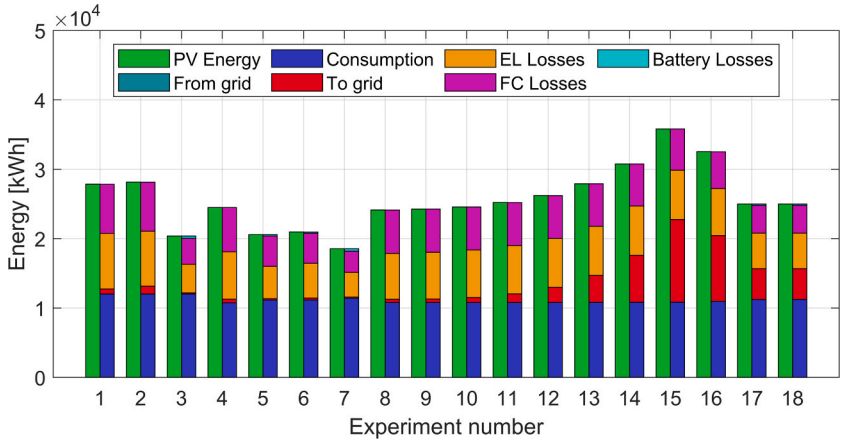

Fig. 19. Annual energy balance for each experiment.

technological components. For comparison, the annual costs of traditional electricity supply from the public grid are also shown for several areas (GE-Germany, SI-Slovenia, IT-Italy, EU average). Fig. 19 illustrates the annual energy balance of each experiment. Electric energy generated by the PV plant covers load consumption (electric loads and the heat pump), electrolyser losses, fuel cell losses, battery losses and electricity supplied to the grid. As explained, electric energy is supplied to the grid only in case when it is temporarily impossible to store excess electricity in the battery or convert it to hydrogen due to storage capacity limitations, electrolyser power limitation, or battery charging power limitation. Note that electricity supplied to the grid actually represents a loss, since the possibility of selling the excess electricity is not considered in this study. Optionally selling the excess electricity would significantly increase the financial viability of the proposed local power system. In all experiments, no electric energy is obtained from the grid and the system is 100 % self-sufficient.

It can be seen that electrolyser and fuel cell losses are significant in cases without the battery. In these cases, the hydrogen system is also used for daily balancing, resulting in high conversion losses. Interestingly, despite having high losses and therefore requiring large amount of generated electricity, Experiment 16 results in the lowest annual energy supply costs. This is due to the absence of battery CAPEX and the relatively small sizes and low CAPEX of the electrolyser and hydrogen storage. In general, low energy conversion losses do not necessarily lead to a low annual energy supply cost. This is also evident from Fig. 20, which shows the energy efficiency achieved during the experiments. It is defined as the ratio between the energy consumed (by electric loads and the heat pump) and the energy generated by the PV plant.

The proposed methodology relies on mathematical modelling and simulation to predict the operational performance of the local energy system. Inevitably, models involve simplifications of the real system, which may result in deviations between simulated and actual operation.

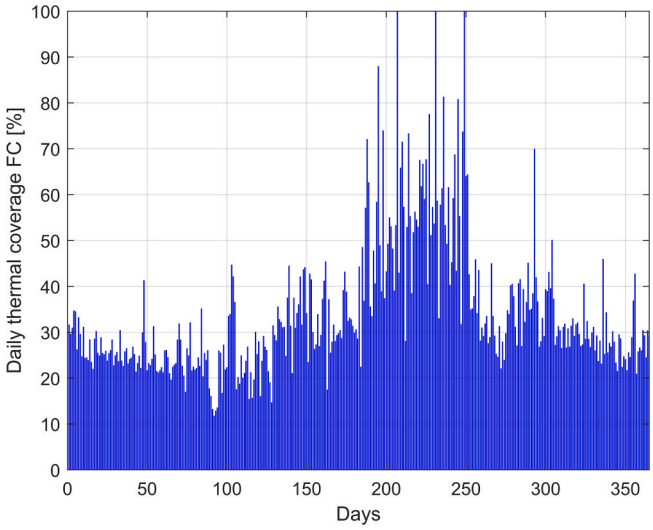

Fig. 21. Contribution of fuel cell thermal losses to total heat demand (Exp. 16 – system without battery).

The degradation of electrochemical components, including the electrolyser, fuel cell, and battery, is represented using simplified degradation models. In practice, degradation rates depend strongly on

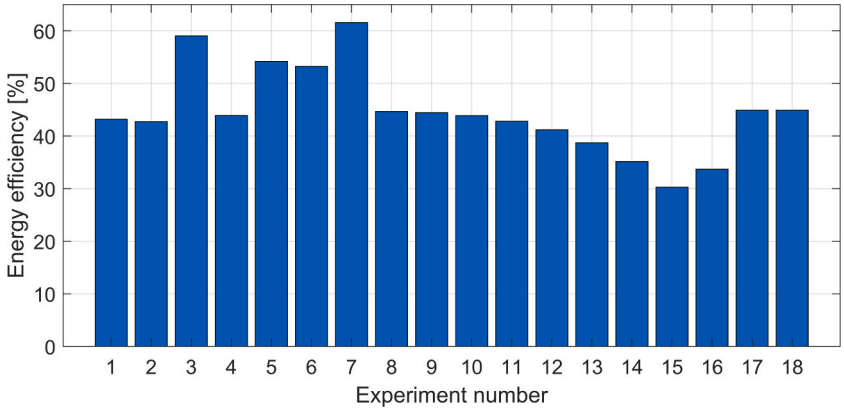

Fig. 20. Energy efficiency for each experiment.

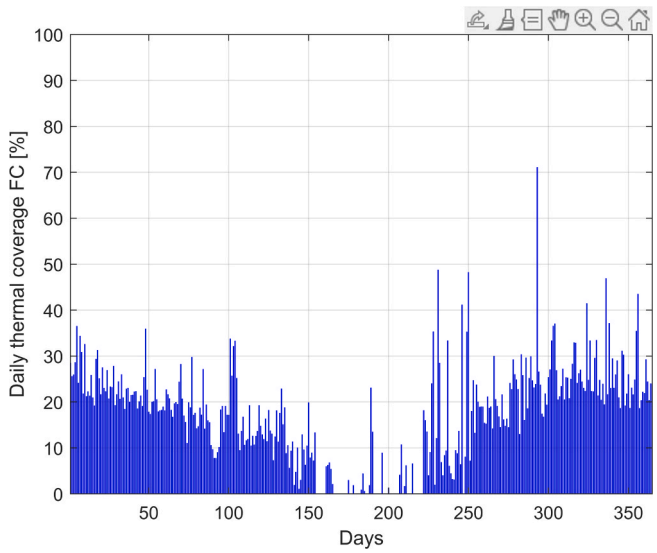

Fig. 22. Contribution of fuel cell thermal losses to total heat demand (Exp. 17 – system with battery).

operating conditions, such as load variability, intermittency, and the frequency of start-up and shutdown events, as well as on the specific technology, manufacturer, and design of each component. Consequently, actual degradation behaviour is difficult to predict accurately and may differ from the assumed scenarios.

Electricity generation from photovoltaic (PV) panels depends on solar irradiance. In this study, future solar radiation is estimated using historical data; however, annual irradiance profiles vary due to unpredictable weather and climatic conditions. Actual PV power output is also affected by site-specific factors, such as micro-location, system orientation, and ambient temperature, which influence PV module efficiency. These factors are not explicitly considered in this analysis, as they are case-dependent and would require detailed site-specific modelling.

The annual costs of electricity and heat supply in the proposed local renewable energy system are determined by the capital and operational costs of its main components. Several key technologies, including the electrolyser, hydrogen storage system, and fuel cell, are not yet manufactured at large-scale and therefore have high specific investment costs. Consequently, the levelised costs of electricity and heat supply are high, limiting the current economic competitiveness of the system compared with conventional energy supply from the public electricity grid. However, significant cost reductions are expected with technological maturation, large-scale deployment, and learning effects, which should improve the system's economic viability in the future.

Higher annual costs of local electricity supply compared to traditional grid supply do not necessarily make local supply unattractive. An interesting recent study [55], based on a survey of 350 participants, shows that despite expert scepticism due to high system costs, households show strong interest in residential hydrogen systems, with some willing to pay up to 24 % higher costs.

6. Conclusions

The paper presents an operational and economic analysis of an energy-independent, self-sustained PV-powered household that uses hydrogen and battery energy storage to balance the mismatch between energy consumption and PV energy generation.

To conduct the study, a model of the entire system was developed. Using this model, a multi-scenario simulation analysis was carried out, highlighting various aspects of the system implementation. Technoeconomic models were built for all components, forming the basis for economic feasibility analysis. Thus, the presented simulation model serves as a design, demonstration, and decision support tool, helping to determine the optimum sizes of system components (such as the PV power plant, hydrogen storage and battery capacity, electrolyser and fuel cell power) and predict the technical and economic outcomes of system operation. This supports the feasibility studies conducted prior to actual investments into hydrogen systems. To further increase the efficiency of this tool, it can be upgraded with an automated optimisation algorithm (e.g. genetic algorithm or particle swarm optimisation), which is the focus of ongoing development. The presented power management algorithm is simple and efficient, but there is potential for improvement, such as by using model predictive control. Another possibility is to enhance the control algorithm to enable hydrogen production using energy stored in the battery. This would allow the use of a smaller electrolyser with lower capital expenditure, while increasing its operating time and utilisation factor. In this paper, simplified degradation models are used for the electrolyser, fuel cell, and battery. To improve the accuracy of the simulations, more detailed degradation models could be developed that account for operating conditions such as load factors, load variation rates, start-stop events, and other relevant stressors.

The results show that energy balancing significantly increases the primary cost of photovoltaic (PV) electric power (by approximately a factor of three), which is unfavourable. Additionally, the pricing structure of the annual electric energy supply indicates that hydrogen storage is a major cost contributor. For the given electricity generation and consumption time profiles, there are two optimal system configurations, one with a battery and one without. The optimal system configuration with a battery (Experiment 17) consists of a 132 m^2 PV plant, a 7 kW electrolyser, a 6 kW fuel cell, 135 kg of hydrogen storage, and a 6 kWh battery. The optimal system configuration without a battery (Experiment 16) comprises a 173 m^2 PV plant, a 7 kW electrolyser, a 6 kW fuel cell, and 130 kg of hydrogen storage. In both cases, the annual electricity supply cost is approximately 4300 EUR.

Both systems may be economically competitive in regions with high electricity and transmission prices, such as Germany, where the annual cost for the same electricity consumption profile is also approximately 4300 EUR. Moreover, anticipated increases in electricity and transmission costs are expected to further increase the competitiveness of local renewable energy systems in other countries. Furthermore, hydrogen system technologies (electrolysers, fuel cells, and hydrogen storage units) are currently not mass-produced, resulting in high costs. Over time, with expected reductions in equipment costs and with potential subsidies, the effect of which is also discussed, such a system could become a green and self-sufficient alternative to conventional public grid-based electricity supply.

CRediT authorship contribution statement

Matic Rutnik: Writing – original draft, Visualization, Validation, Software, Methodology, Investigation, Formal analysis, Data curation, Conceptualization. **Boštjan Pregelj:** Writing – review & editing. **David Jovan:** Writing – review & editing. **Gregor Dolanc:** Writing – review & editing, Supervision, Resources, Project administration, Funding acquisition.

Declaration of competing interest

The authors declare the following financial interests/personal relationships which may be considered as potential competing interests: Matic Rutnik reports financial support was provided by Slovenian Research and Innovation Agency. If there are other authors, they declare that they have no known competing financial interests or personal relationships that could have appeared to influence the work reported in this paper.

Acknowledgments

This work was supported by the research programme P2-0001 and research project L2-4456, both funded by the Slovenian Research and Innovation Agency, and by research project HyBReED, funded by the European Commission (NextGenerationEU) and Slovenian Research and Innovation Agency (contract number TN-03-0104). The support is gratefully acknowledged.

Appendix A. Supplementary data

Supplementary data to this article can be found online at https://doi.org/10.1016/j.enconman.2026.121244.

Data availability

The complete implementation, including all scripts and simulations, is publicly available on GitHub:https://github.com/maticrutnik-hub/Green-hydrogen.

References

[1] Vartiainen E, Breyer C, Moser D, Medina ER. True cost of solar hydrogen. Sol RRL 2021. https://doi.org/10.1002/solr.202100487.
[2] Kleinebrahm M, Weinand JM, Naber E, McKenna R, Ardone A, Fichtner W. Two million European single-family homes could abandon the grid by 2050. Joule 2023; 7(11):2485–510. https://doi.org/10.1016/j.joule.2023.09.012.
[3] Braungardt S, Tezak B, Rosenow J, Bürger V. Banning boilers: an analysis of existing regulations to phase out fossil fuel heating in the EU. Renew Sustain Energy Rev 2023;183:113442. https://doi.org/10.1016/j.rser.2023.113442.
[4] Soto EA, Bosman LB, Wollega E, Leon-Salas WD. Comparison of net-metering with peer-to-peer models using the grid and electric vehicles for the electricity exchange. Appl Energy 2022;310:118562. https://doi.org/10.1016/j.apenergy.2022.118562.
[5] Khalid F, Dincer I, Rosen MA. Analysis and assessment of an integrated hydrogen energy system. Int J Hydrogen Energy 2016;41(19):7960–7. https://doi.org/10.1016/j.ijhydene.2015.12.221.
[6] Puranen P, Kosonen A, Ahola J. Technical feasibility evaluation of a solar PV based off-grid domestic energy system with battery and hydrogen energy storage in northern climates. Sol Energy 2021;213:246–59. https://doi.org/10.1016/j.solener.2020.10.089.
[7] Keiner D, Thoma C, Bogdanov D, Breyer C. Seasonal hydrogen storage for residential on- and off-grid solar photovoltaics prosumer applications: revolutionary solution or niche market for the energy transition until 2050? Appl Energy 2023;340:121009. https://doi.org/10.1016/j.apenergy.2023.121009.
[8] Marocco P, Ferrero D, Lanzini A, Santarelli M. The role of hydrogen in the optimal design of off-grid hybrid renewable energy systems. J Energy Storage 2022;46: 103893. https://doi.org/10.1016/j.est.2021.103893.
[9] M. Steilen and L. Jörissen, Hydrogen conversion into electricity and thermal energy by fuel cells: use of H2-systems and batteries, in electrochemical energy storage for renewable sources and grid balancing, P. T. Moseley and J. Garche, Eds. Elsevier, pp. 143–158, 2015, https://doi.org/10.1016/B978-0-444-62616-5.00010-3.
[10] Bogdanov D, et al. Low-cost renewable electricity as the key driver of the global energy transition towards sustainability. Energy 2021;227:120467. https://doi.org/10.1016/j.energy.2021.120467.
[11] Lagorse J, Simões MG, Miraoui A, Costerg P. Energy cost analysis of a solar-hydrogen hybrid energy system for stand-alone applications. Int J Hydrogen Energy 2008;33(12):2871–9. https://doi.org/10.1016/j.ijhydene.2008.03.054.
[12] Castañeda M, Cano A, Jurado F, Sánchez H, Fernández LM. Sizing optimization, dynamic modeling and energy management strategies of a stand-alone PV/hydrogen/battery-based hybrid system. Int J Hydrogen Energy 2013;38(10): 3830–45. https://doi.org/10.1016/j.ijhydene.2013.01.080.
[13] L. Abdolmaleki and U. Berardi, Hybrid solar energy systems with hydrogen and electrical energy storage for a single house and a midrise apartment in North America, Int J Hydrogen Energy, 52, pt. D, 1381–1394, 2024, https://doi.org/10.1016/j.ijhydene.2023.11.222.
[14] Ancona MA, Catena F, Ferrari F. Optimal design and management for hydrogen and renewables based hybrid storage micro-grids. Int J Hydrogen Energy 2023;48 (54):20844–60. https://doi.org/10.1016/j.ijhydene.2022.10.204.
[15] Maleki A, Pourfayaz F. Optimal sizing of autonomous hybrid photovoltaic/wind/battery power system with LPSP technology by using evolutionary algorithms. Sol Energy 2015;115:471–83. https://doi.org/10.1016/j.solener.2015.03.004.
[16] Mohammed A, Ghaithan AM, Al-Hanbali A, Attia AM. A multi-objective optimization model based on mixed integer linear programming for sizing a hybrid PV-hydrogen storage system. Int J Hydrogen Energy 2023;48(26):9748–61. https://doi.org/10.1016/j.ijhydene.2022.12.060.
[17] Yang G, Zhang H, Wang W, Liu B, Lyu C, Yang D. Capacity optimization and economic analysis of PV–hydrogen hybrid systems with physical solar power curve modeling. Energy Convers Manag 2023;288. https://doi.org/10.1016/j.enconman.2023.117128.
[18] Zhang W, Maleki A, Rosen MA, Liu J. Optimization with a simulated annealing algorithm of a hybrid system for renewable energy including battery and hydrogen storage. Energy 2018;163:191–207. https://doi.org/10.1016/j.energy.2018.08.112.
[19] Singh A, Baredar P, Gupta B. Techno-economic feasibility analysis of hydrogen fuel cell and solar photovoltaic hybrid renewable energy system for academic research building. Energy Convers Manag 2017;145:398–414. https://doi.org/10.1016/j.enconman.2017.05.014.
[20] Yang P, Nehorai A. Joint optimization of hybrid energy storage and generation capacity with renewable energy. IEEE Trans Smart Grid July 2014;5(4):1566–74. https://doi.org/10.1109/TSG.2014.2313724.
[21] Wang J, Xue K, Guo Y, Ma J, Zhou X, Liu M, et al. Multi-objective capacity programming and operation optimization of an integrated energy system considering hydrogen energy storage for collective energy communities. Energ Conver Manage 2022;268:116057. https://doi.org/10.1016/j.enconman.2022.116057.
[22] Fan G, Liu Z, Liu X, Shi Y, Wu D, Guo J, et al. Energy management strategies and multi-objective optimization of a near-zero energy community energy supply system combined with hybrid energy storage. Sustain Cities Soc 2022;83:103970. https://doi.org/10.1016/j.scs.2022.103970.
[23] Soyturk G, Cetinkaya SA, Yekta MA, Joghan MMK, Mohebi H, Kizilkan O, et al. Dynamic analysis and multi-objective optimization of solar and hydrogen energy-based systems for residential applications: a review. Int J Hydrogen Energy 2024; 75:662–89. https://doi.org/10.1016/j.ijhydene.2024.05.095.
[24] Wang C, Nehrir MH. Power management of a stand-alone wind/photovoltaic/fuel cell energy system. IEEE Trans Energy Convers Sept. 2008;23(3):957–67. https://doi.org/10.1109/TEC.2007.914200.
[25] Behzadi MS, Niasati M. Comparative performance analysis of a hybrid PV/FC/battery stand-alone system using different power management strategies and sizing approaches. Int J Hydrogen Energy 2015;40(1):538–48. https://doi.org/10.1016/j.ijhydene.2014.10.097.
[26] Vosen SR, Keller JO. Hybrid energy storage systems for stand-alone electric power systems: optimization of system performance and cost through control strategies. Int J Hydrogen Energy 1999;24(12):1139–56. https://doi.org/10.1016/S0360-3199(98)00175-X.
[27] Sossan F, Bindner H, Madsen H, Torregrossa D, Chamorro LR, Paolone M. A model predictive control strategy for the space heating of a smart building including cogeneration of a fuel cell-electrolyzer system. Int J Electr Power Energy Syst 2014; 62:879–89. https://doi.org/10.1016/j.ijepes.2014.05.040.
[28] Chávez-Ramírez AU, Vallejo-Becerra V, Cruz JC, Ornelas R, Orozco G, Muñoz-Guerrero R, et al. A hybrid power plant (Solar–Wind–Hydrogen) model based in artificial intelligence for a remote-housing application in Mexico. Int J Hydrogen Energy 2013;38(6):2641–55. https://doi.org/10.1016/j.ijhydene.2012.11.140.
[29] Rouholamini M, Mohammadian M. Energy management of a grid-tied residential-scale hybrid renewable generation system incorporating fuel cell and electrolyzer. Energ Buildings 2015;102:406–16. https://doi.org/10.1016/j.enbuild.2015.05.046.
[30] Mehrjerdi H. Peer-to-peer home energy management incorporating hydrogen storage system and solar generating units. Renew Energy 2020;156:183–92. https://doi.org/10.1016/j.renene.2020.04.090.
[31] Heidarnejad P, Fathi P, Karami M. Thermoeconomic modeling and artificial neural network-based optimization of a decarbonized combined heat and power plant with hydrogen re-electrification. Int J Hydrogen Energy 2025. https://doi.org/10.1016/j.ijhydene.2025.01.486.
[32] Enaloui R, Sharifi S, Faridpak B, Hammad A, Al-Hussein M, Musilek P. Techno-economic assessment of a solar-powered green hydrogen storage concept based on reversible solid oxide cells for residential micro-grid: a case study in Calgary. Energy 2025;319:134981. https://doi.org/10.1016/j.energy.2025.134981.
[33] Xu X, Wang B, Shi M, Li G, Zhang Y, Wang Q, et al. Research on hydrogen storage system configuration and optimization in regional integrated energy systems considering electric-gas-heat-hydrogen integrated demand response. Int J Hydrogen Energy 2025;135:86–103. https://doi.org/10.1016/j.ijhydene.2025.04.512.
[34] Huang Y, Ahmed S, Ueda S, Liang X, Howlader HOR, Lotfy ME, et al. Operation optimization of combined Heat and Power microgrid in buildings consider renewable energy, electric vehicles and hydrogen fuel. Energy 2025;319:134690. https://doi.org/10.1016/j.energy.2025.134690.
[35] Nasser M, Hassan H. Assessment of hydrogen production from waste heat using hybrid systems of Rankine cycle with proton exchange membrane/solid oxide electrolyzer. Int J Hydrogen Energy 2023;48(20):7135–53. https://doi.org/10.1016/j.ijhydene.2022.11.187.
[36] Cheng J, Yang F, Zhang H, Wang N, Yan Y, Xu Y. A multi-level optimization design and intelligent control framework for fuel cell-based combined heat and power systems. Energy Convers Manag 2025;325:119397. https://doi.org/10.1016/j.enconman.2024.119397.
[37] Abe JO, Popoola API, Ajenifuja E, Popoola OM. Hydrogen energy, economy and storage: review and recommendation. Int J Hydrogen Energy 2019;44(29): 15072–86. https://doi.org/10.1016/j.ijhydene.2019.04.068.
[38] Slovenian Environment Agency – ARSO, solar irradiation data (archive in Slovene language), https://meteo.arso.gov.si/met/sl/archive/.
[39] T. Brudermueller, E. Fleisch, M. G. Vayá, T. Staake, HEAPO – an open dataset for heat pump optimization with smart electricity meter data and on-site inspection protocols, E-Energy '25: Proceedings of the 16th ACM International Conference on

Future and Sustainable Energy Systems, pp. 699 – 711, https://doi.org/10.1145/3679240.3734637.
[40] Capuano M, Sorrentino M, Agelin-Chaab M. Design and analysis of a hybrid space heating system based on HT-PEM fuel cell and an air source heat pump with a novel heat recovery strategy. Appl Therm Eng 2023;231:120947. https://doi.org/10.1016/j.applthermaleng.2023.120947.
[41] Eurostat - Electricity prices components for household consumers - annual data, https://ec.europa.eu/eurostat/databrowser/view/nrg_pc_204_c__custom_18132840/default/table.
[42] Santos Andrade T, Ramakrishna SKN, Thiringer T. Integrating a fuel cell with a heat pump: an energy-saving system for residential housing. Energ Conver Manage 2025;326:119509. https://doi.org/10.1016/j.enconman.2025.119509.
[43] R. Elkhatib, T. Kaoutari, H. Louahlia, Green hydrogen energy source for a residential fuel cell micro-combined heat and power, Appl Thermal Eng, 248, Part A, 123194, 2024, https://doi.org/10.1016/j.applthermaleng.2024.123194.
[44] Gabana P, Reyes M, Tinaut FV, Novella R. A 4E analysis of different fuel Cell mCHP configurations operating with different strategies in residential applications. Int J Hydrogen Energy 2025;144:1051–69. https://doi.org/10.1016/j.ijhydene.2025.02.377.
[45] Marocco P, Ferrero D, Lanzini A, Santarelli M. Optimal design of stand-alone solutions based on RES + hydrogen storage feeding off-grid communities. Energ Conver Manage 2021;238:114147. https://doi.org/10.1016/j.enconman.2021.114147.
[46] VR Rikka, SR Sahu, A Chatterjee, R Prakash, G Sundararajan, R Gopalan, Enhancing cycle life and usable energy density of fast charging LiFePO4-graphite cell by regulating electrodes' lithium level, iScience, Volume 25, Issue 9, 2022, https://doi.org/10.1016/j.isci.2022.104831.
[47] Ellis B, White C, Swan L. Degradation of lithium-ion batteries that are simultaneously servicing energy arbitrage and frequency regulation markets. J Storage Mater 2023;66:107409. https://doi.org/10.1016/j.est.2023.107409.
[48] Cozzolino R, Bella G. A review of electrolyzer-based systems providing grid ancillary services: current status, market, challenges and future directions. Front Energy Res 2024;12. https://doi.org/10.3389/fenrg.2024.1358333.
[49] Elmamoun S, El Maakoul A, Bouhssine Z, Bouramdane A-A, Degiovanni A. Performance analysis of a fuel cell-based combined heating, cooling, and power system for a residential building: a case study in Morocco. Energ Conver Manage 2024;321:119067. https://doi.org/10.1016/j.enconman.2024.119067.
[50] Huang Z, Shen J, Chan SH, Tu Z. Transient response of performance in a proton exchange membrane fuel cell under dynamic loading. Energ Conver Manage 2020;226. https://doi.org/10.1016/j.enconman.2020.113492.
[51] Esposito L, van der Wiel M, Acar C. Hydrogen storage solutions for residential heating: a thermodynamic and economic analysis with scale-up potential. Int J Hydrogen Energy 2024;79:579–93. https://doi.org/10.1016/j.ijhydene.2024.06.279.
[52] van der Roest E, Bol R, Fens T, van Wijk A. Utilisation of waste heat from PEM electrolysers – unlocking local optimisation. Int J Hydrogen Energy 2023;48(72):27872–91. https://doi.org/10.1016/j.ijhydene.2023.03.374.
[53] Commission E. STAYERS – stationary PEM fuel cells with improved Durability for Extended Service (FP7 STAYERS Project Report, GA 256721). Available from CORDIS repository 2014. https://cordis.europa.eu/project/id/256721/reporting.
[54] Möller MC, Krauter S. Hybrid energy system model in Matlab/Simulink based on solar energy, lithium-ion battery and hydrogen, Energies, volume 15. Pages 2022;2201. https://doi.org/10.3390/en15062201.
[55] A-L Klingler, J Dörr, Hydrogen micro-systems: households' preferences and economic futility. Energies, 17, 1524, 2024, https://doi.org/10.3390/en17071524.
[56] Arsalis A, Kær SK, Nielsen MP. Modeling and optimization of a heat-pump-assisted high temperature proton exchange membrane fuel cell micro-combined-heat-and-power system for residential applications. Appl Energy 2015;147:569–81. https://doi.org/10.1016/j.apenergy.2015.03.031.